THE INDUSTRIAL ELECTRONICS HANDBOOK

Editor-in-Chief
J. DAVID IRWIN

CRC PRESS
IEEE PRESS

A CRC Handbook Published in Cooperation with IEEE Press

Kenjo, Takashi, 1984. *Stepping Motors and Their Microprocessor Controls*, Oxford Science Publications, Oxford, UK.
SGS 1987. *SGS Motion Control Application Manual.*

53.7 Control

Fathi Ghorbel

Introduction

The motion control problem of robot manipulators consists of devising an appropriate control law that causes the joint variables to follow a prescribed trajectory making the end effector execute a specific task. Over the past decade, there has been a lot of progress in this area. Serial link (open kinematic chain) robot manipulators in particular have attracted the attention of many control/dynamics researchers which resulted in a remarkable rich and rigorous body of trajectory control results that range from the well known and simple independent-joint control laws, to more advanced robust and adaptive nonlinear techniques.

Several aspects of the motion control problem have been addressed in the literature including robustness of trajectory control strategies with respect to joint flexibility, link flexibility, and environment stiffness. Recent publication covering recent advances in this area include Spong and Vidyasagar (1989), Spong et al. (1993), and Lewis et al. (1993). In particular, the recent surveys of Ortega and Spong (1988) and Abdallah et al. (1991) review several adaptive and robust control strategies.

The purpose of this section is to describe and illustrate the use of some of the recent control strategies. An emphasis has been made to show how the structural properties of the equations of motion of robot manipulators play an important role in devising appropriate control laws. Examples have been used to illustrate different aspects of the topic and to show application of the results. Experimental results have been included to evaluate the performance of one particular control law.

Equations of Motion

Degrees of Freedom and Generalized Coordinates

Two important characteristics of a robot manipulator are the number of degrees of freedom (DOF) and the generalized coordinates. The number of DOF is defined as the number of coordinates which are used to specify the configuration of the manipulator minus the number of independent equations of constraints. It is a characteristic of the robot itself and does not depend upon the particular set of coordinates used to describe the robot's configuration. The configuration of the planar one-link manipulator shown in Figure 53.58 is fully specified by the coordinates x_A and y_A of point A in the x-y coordinate system, and the angle θ measured from the x axis to the axis passing through point A and the center of mass of the link. Let the link be constrained to rotate about an axis normal to the x-y plane passing through point A. The two equations describing the constraints are $x_A = x^*$ and $y_A = y^*$ where x^* and y^* are fixed

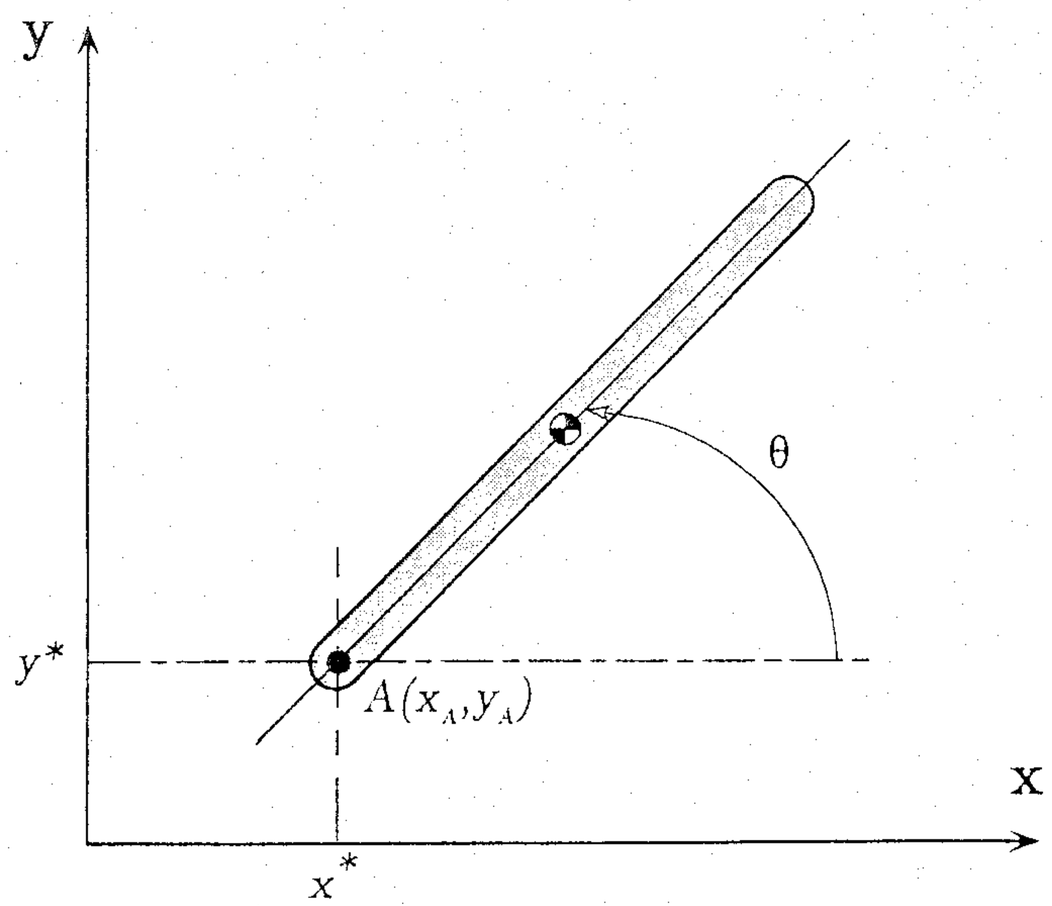

Figure 53.58 A one-link manipulator.

coordinates. The planar one-link manipulator has three configuration coordinates and two constraint equations. Consequently, it has one degree of freedom.

Any set of parameters which unambiguously represent the configuration of the manipulator can serve as a system of coordinates in a more general sense. Such parameters are known as generalized coordinates. The angle θ in Figure 53.58 serves as a generalized coordinate for the one-link manipulator.

Euler-Lagrange Equations of Robot Manipulators

A well known method to derive the equations of motion of mechanical systems is the use of the Euler-Lagrange equations (Greenwood, 1977)

$$\frac{d}{dt}\frac{\partial L}{\partial \dot{\mathbf{q}}} - \frac{\partial L}{\partial \mathbf{q}} = \mathbf{u}$$

where for an n-DOF manipulator, $\mathbf{q} = [q_1, q_2, \cdots, q_n]^T$ is the vector of generalized coordinates of the system, the Lagrangian $L = K - P$ is the sum of the kinetic energy K and the potential energy P of the manipulator, and $\mathbf{u} = [u_1, u_2, \cdots, u_n]^T$ is the vector of generalized forces driving the system.

An n-DOF robot manipulator has two special features (Spong and Vidyasagar, 1989): First, the potential energy $P = P(\mathbf{q})$ is independent of the generalized velocity vector $\dot{\mathbf{q}}$, Second, the kinetic energy is a quadratic function of $\dot{\mathbf{q}}$,

$$K = \sum_{i=1}^{n}\sum_{j=1}^{n}\frac{1}{2}d_{ij}(\mathbf{q})\dot{q}_i\dot{q}_j$$

$$\stackrel{\Delta}{=} \frac{1}{2}\dot{\mathbf{q}}^T D(\mathbf{q})\dot{\mathbf{q}},$$

where $D(\mathbf{q})$ is an $n \times n$ matrix called the inertia matrix. Application of the Euler-Lagrange equations to the case of n-DOF robot

manipulator results in the following equation (Spong and Vidyasagar, 1989)

$$\sum_{j=1}^{n} d_{kj}(\mathbf{q})\ddot{q}_j + \sum_{i=1}^{n}\sum_{j=1}^{n} c_{ijk}(\mathbf{q})\dot{q}_i\dot{q}_j + \phi_k(\mathbf{q}) = u_k, \quad (53.14)$$

$$k = 1, 2, \ldots, n.$$

where

$$c_{ijk} = \frac{1}{2}\left\{\frac{\partial d_{kj}}{\partial q_i} + \frac{\partial d_{ki}}{\partial q_j} - \frac{\partial d_{ij}}{\partial q_k}\right\}$$

are known as the Christoffel symbols, and

$$\phi_k = \frac{\partial P}{\partial q_k}.$$

We commonly write the equations of motion (Equation 53.14) in matrix form in the following manner

$$D(\mathbf{q})\ddot{\mathbf{q}} + C(\mathbf{q}, \dot{\mathbf{q}})\dot{\mathbf{q}} + \mathbf{g}(\mathbf{q}) = \mathbf{u}, \quad (53.15)$$

where the vector $\mathbf{g}(\mathbf{q}) = [\phi_1, \phi_2, \cdots, \phi_n]^T$, and the elements c_{kj} of the matrix $C(\mathbf{q}, \dot{\mathbf{q}})$ are defined here as

$$c_{kj} = \sum_{i=1}^{n} c_{ijk}(\mathbf{q})\dot{q}_i$$

$$= \sum_{i=1}^{n} \frac{1}{2}\left\{\frac{\partial d_{kj}}{\partial q_i} + \frac{\partial d_{ki}}{\partial q_j} - \frac{\partial d_{ij}}{\partial q_k}\right\}\dot{q}_i. \quad (53.16)$$

Note that other choices of the $C(\mathbf{q},\dot{\mathbf{q}})$ matrix are possible.

EXAMPLE 53.1 (Spong and Vidyasagar, 1989):

Consider the planar two-DOF two-link manipulator depicted in Figure 53.59 where for $i = 1, 2$, m_i is the mass of link i, l_i denotes the length of link i, l_i is the distance from the previous joint to the center of mass of link i, and I_i denotes the moment of inertia of link i about an axis perpendicular to the page and passing through the center of mass of link i. Let the generalized coordinates be $\mathbf{q} = [q_1, q_2]^T$. The computation of the kinetic energy is usually facilitated by setting an appropriate coordinate system to describe the kinematic relationships. For robot manipulators, the Denavit-Hartenberg convention is commonly used for this purpose (Spong and Vidyasagar, 1989). In fact, the kinetic energy for this example is given by

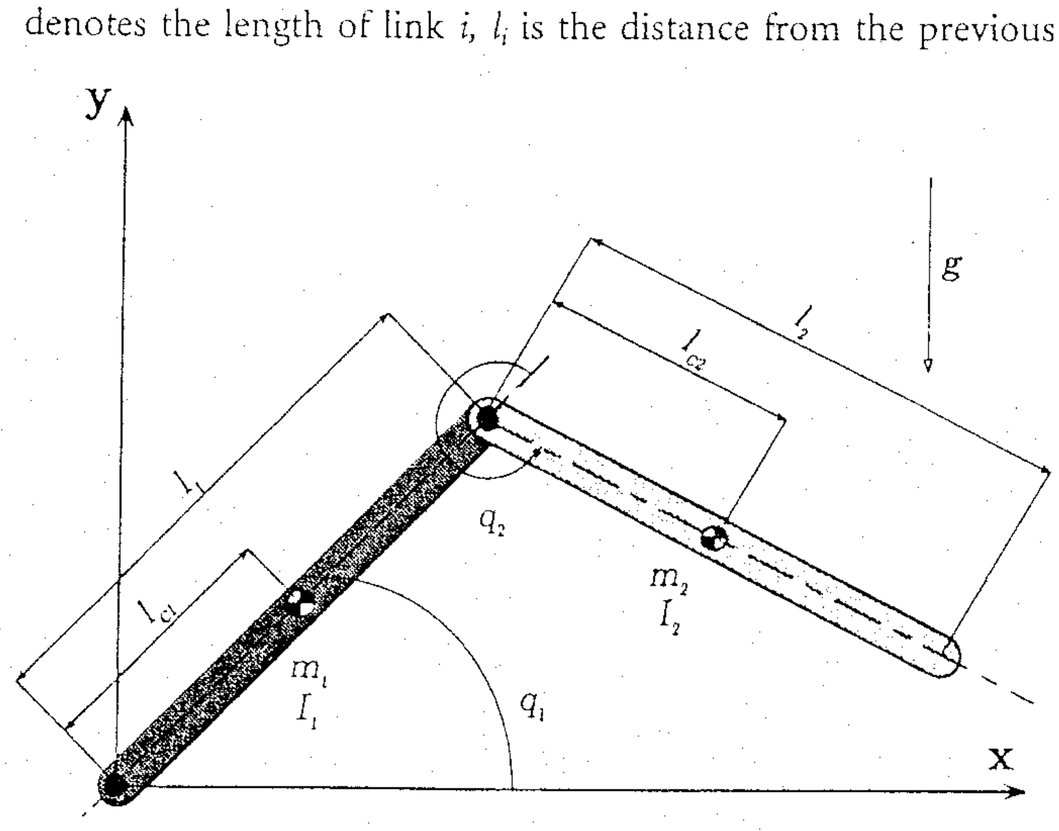

Figure 53.59 A planar two-link manipulator.

$$K = \frac{1}{2}\dot{\mathbf{q}}^T D(\mathbf{q})\dot{\mathbf{q}}$$

where the elements of $D(\mathbf{q})$, namely d_{ij}, $i, j = 1, 2$, satisfy

$$d_{11} = m_1 l_{c1}^2 + m_2(l_1^2 + l_{c2}^2 + 2l_1 l_{c2}\cos q_2) + I_1 + I_2$$

$$d_{12} = d_{21} = m_2(l_{c2}^2 + l_1 l_{c2}\cos q_2) + I_2$$

$$d_{22} = m_2 l_{c2}^2 + I_2.$$

The Christoffel symbols are therefore computed as follows:

$$c_{111} = \frac{1}{2}\frac{\partial d_{11}}{\partial q_1} = 0$$

$$c_{121} = c_{211} = \frac{1}{2}\frac{\partial d_{11}}{\partial q_2} = -m_2 l_1 l_{c2}\sin q_2$$

$$c_{221} = \frac{\partial d_{12}}{\partial q_2} - \frac{1}{2}\frac{\partial d_{22}}{\partial q_1} = -m_2 l_1 l_{c2}\sin q_2$$

$$c_{112} = \frac{\partial d_{21}}{\partial q_1} - \frac{1}{2}\frac{\partial d_{11}}{\partial q_2} = m_2 l_1 l_{c2}\sin q_2$$

$$c_{122} = c_{212} = \frac{1}{2}\frac{\partial d_{22}}{\partial q_1} = 0$$

$$c_{222} = \frac{1}{2}\frac{\partial d_{22}}{\partial q_2} = 0.$$

The potential energy of the two-link manipulator is the sum of the potential energy of each individual link so that

$$P(\mathbf{q}) = m_1 g l_{c1}\sin q_1 + m_2 g(l_1\sin q_1 + l_{c2}\sin(q_1 + q_2))$$

$$= (m_1 l_{c1} + m_2 l_1)g\sin q_1 + m_2 g l_{c2}\sin(q_1 + q_2),$$

where g is the gravitational acceleration. It follows that

$$\phi_1 = \frac{\partial P}{\partial q_1} = (m_1 l_{c1} + m_2 l_1)g\cos q_1 + m_2 g l_{c2}\cos(q_1 + q_2)$$

$$\phi_2 = \frac{\partial P}{\partial q_2} = m_2 g l_{c2}\cos(q_1 + q_2).$$

We now write the equations of motion in vector form (see Equation 53.15) using (Equation 53.16) for the computation of the matrix $C(\mathbf{q}, \dot{\mathbf{q}})$:

$$D(\mathbf{q}) = \begin{bmatrix} m_1 l_{c1}^2 + m_2(l_1^2 + l_{c2}^2 + 2l_1 l_{c2}\cos q_2) + I_1 + I_2 & m_2(l_{c2}^2 + l_1 l_{c2}\cos q_2) + I_2 \\ m_2(l_{c2}^2 + l_1 l_{c2}\cos q_2) + I_2 & m_2 l_{c2}^2 + I_2 \end{bmatrix},$$

$$C(\mathbf{q}, \dot{\mathbf{q}}) = \begin{bmatrix} -m_2 l_1 l_{c2}\sin q_2 \dot{q}_2 & -m_2 l_1 l_{c2}\sin q_2(\dot{q}_1 + \dot{q}_2) \\ m_2 l_1 l_{c2}\sin q_2 \dot{q}_1 & 0 \end{bmatrix},$$

$$\mathbf{g}(\mathbf{q}) = \begin{bmatrix} (m_1 l_{c1} + m_2 l_1)g\cos q_1 + m_2 g l_{c2}\cos(q_1 + q_2) \\ m_2 g l_{c2}\cos(q_1 + q_2) \end{bmatrix}.$$

Structural Properties of the Equations of Motion

Even though the equations of motion (Equation 53.15) of an n-DOF robot manipulator are generally very complex nonlinear differential equations, they have interesting structural properties which are exploited to facilitate control law design. We discuss four properties. First, the inertia matrix $D(\mathbf{q})$ is symmetric so that for each $\mathbf{q}$, $d_{ij}(\mathbf{q}) = d_{ji}(\mathbf{q})$, $i,j = 1,2,\cdots,n$. It is also positive definite meaning that all of the eigenvalues of $D(\mathbf{q})$ are strictly positive for any given $\mathbf{q}$, or equivalently, for each non-zero vector $\mathbf{x}$ of the same dimension as $\mathbf{q}$, the scalar $\mathbf{x}^T D(\mathbf{q})\mathbf{x}$ is strictly positive for any given $\mathbf{q}$. Consequently, the inertia matrix $D(\mathbf{q})$ and its inverse $D^{-1}(\mathbf{q})$ are bounded for any given $\mathbf{q}$. In Example 53.1, it is clear that the inertia matrix $D(q_2)$ is symmetric. It is also positive definite which can be easily verified by plotting the eigenvalues of $D(q_2)$ as q_2 varies. Second, there is an independent control input for each DOF. Third, all of the constant parameters of interest such as link masses, moments of inertia, link lengths, etc., appear in the equations of motion as coefficients of functions of the generalized coordinates. These coefficients consist of algebraic combinations of the parameters. By defining each coefficient as a new parameter θ_i, it is possible to write the equations of motion linear with respect to these parameters as follows:

$$D(\mathbf{q})\ddot{\mathbf{q}} + C(\mathbf{q}, \dot{\mathbf{q}})\dot{\mathbf{q}} + \mathbf{g}(\mathbf{q}) = Y(\mathbf{q}, \dot{\mathbf{q}}, \ddot{\mathbf{q}})\Theta = \mathbf{u} \qquad (53.17)$$

where $\mathbf{Y}(\mathbf{q}, \dot{\mathbf{q}}, \ddot{\mathbf{q}})$ is an $n \times r$ matrix of known functions, usually referred to as the regressor, and Θ is a vector of parameters of dimension r. In reference to Example 53.1, we define

$$\Theta^T = [\theta_1\ \theta_2\ \theta_3\ \theta_4\ \theta_5\ \theta_6\ \theta_7\ \theta_8\ \theta_9]$$

$$= [m_1 l_{c1}^2\ m_2 l_1^2\ m_2 l_{c2}^2\ m_2 l_1 l_{c_2}\ I_1\ I_2\ m_1 l_{c_1} g\ m_2 l_1 g\ m_2 l_{c_2} g],$$

$$\mathbf{Y}(\mathbf{q}, \dot{\mathbf{q}}, \ddot{\mathbf{q}}) = [Y_1\ Y_2],$$

$$\mathbf{Y}_1 = \begin{bmatrix} \ddot{q}_1 & \dot{q}_2 & \dot{q}_1 + \dot{q}_2 & 2\mathscr{C}_2\ddot{q}_1 + \mathscr{C}_2\ddot{q}_2 - 2\mathscr{S}_2\dot{q}_1\dot{q}_2 - \mathscr{S}_2\dot{q}_2^2 \\ 0 & 0 & \ddot{q}_1 + \ddot{q}_2 & \mathscr{S}_2\ddot{q}_1 + \mathscr{S}\mathscr{S}_2 \end{bmatrix},$$

$$\mathbf{Y}_2 = \begin{bmatrix} \ddot{q}_1 & \dot{q}_1 + \dot{q}_2 & \mathscr{C}_1 & \mathscr{C}_1 & \mathscr{C}_{12} \\ \ddot{q}_2 & \ddot{q}_2 & 0 & 0 & \mathscr{C}_{12} \end{bmatrix},$$

where $\mathscr{C}_i = \cos q_i$, $i = 1, 2$, and $\mathscr{C}_{12} = \cos(q_1 + q_2)$ and $\mathscr{S}_2 = \sin \mathbf{q}$. Note that the choice of the parameter vector Θ is not unique and the dimension of the parameter space depends on the particular choice of parameters. Fourth, define the matrix $\mathcal{N}(\mathbf{q}, \dot{\mathbf{q}}) = \dot{D}(\mathbf{q}, \dot{\mathbf{q}}) - 2\mathscr{C}(\mathbf{q}, \dot{\mathbf{q}})$. Then $\mathcal{N}$ is skew symmetric meaning that the components n_{jk} of $\mathcal{N}(\mathbf{q}, \dot{\mathbf{q}},)$ satisfy $n_{jk} = -n_{kj}$. Consequently, for any vector $\mathbf{x}$, the scalar $\mathbf{x}^T\mathcal{N}\mathbf{x} = 0$. In Example 53.1,

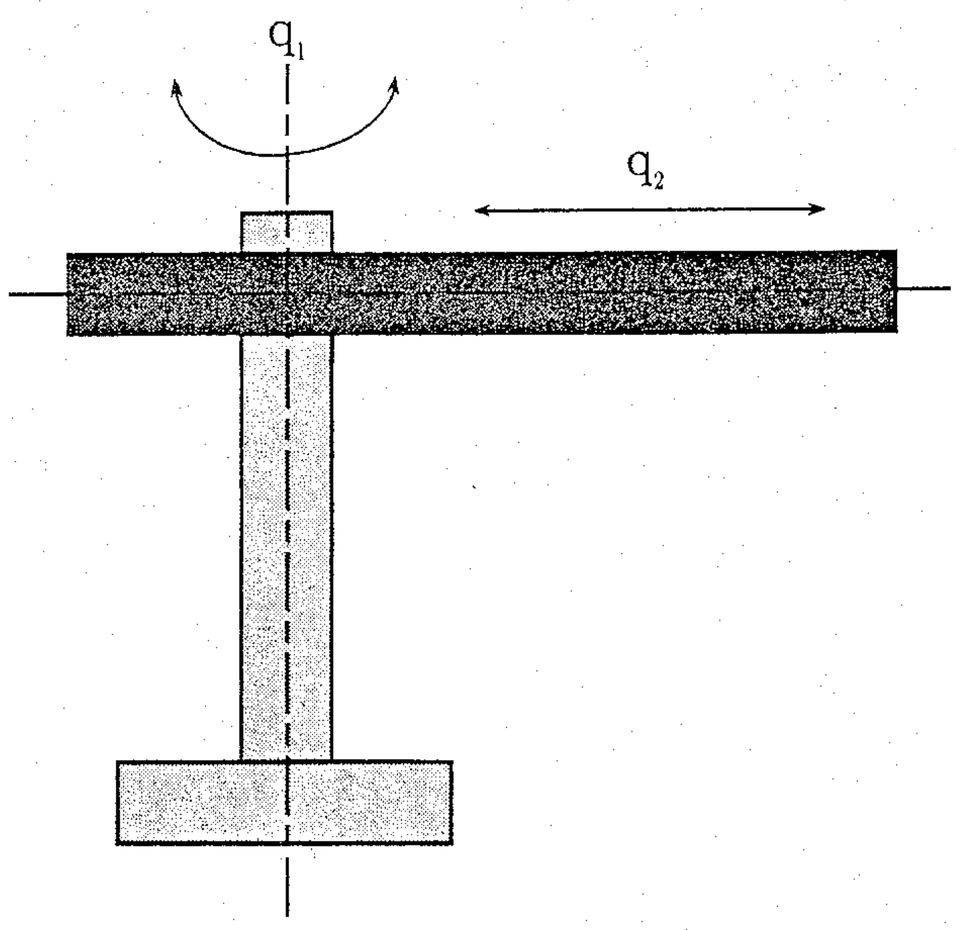

Figure 53.60 A Two DOF manipulator with unbounded inertia matrix.

$$\mathcal{N} = \dot{D} - 2\mathscr{C} = \begin{bmatrix} 0 & m_2 l_1 l_{c_2}\mathscr{S}_2(\dot{q}_2 + 2\dot{q}_1) \\ -m_2 l_1 l_{c_2}\mathscr{S}_2(\dot{q}_2 + 2\dot{q}_1) & 0 \end{bmatrix}$$

which is clearly skew symmetric.

Uniform Boundedness of the Inertia Matrix

The uniform boundedness of the inertia matrix is a typical assumption used in the design and analysis of several modern control laws for robot manipulators as will be demonstrated later. The inertia matrix $D(\mathbf{q})$ is said to be bounded if for each element $d_{ij}(\mathbf{q})$ of $D(\mathbf{q})$, there exists a constant $c < \infty$ such that $|d_{ij}(\mathbf{q})| \leq c$ for all $\mathbf{q}$. $D(\mathbf{q})$ is unbounded if at least one of its elements is not bounded. An important uniform boundedness inequality that is widely used in the robot control literature is

$$0 < \sigma_1 \leq \|D(\mathbf{q})\| \leq \sigma_2 < \infty, \qquad (53.18)$$

where σ_1 and σ_2 are positive constants, and the matrix norm $\|D(\mathbf{q})\| = \sqrt{\lambda_{\max}[D^T(\mathbf{q})D(\mathbf{q})]}$, that is, the square root of the maximum eigenvalue of $[D^T(\mathbf{q})D(\mathbf{q})]$.

It is easy to find robot manipulators which do not satisfy inequality (Equation 53.18). A simple example, shown in Figure 53.60, is that of a two-DOF manipulator with one revolute joint followed by a prismatic joint. The corresponding inertia matrix is

$$D(q_2) = \begin{bmatrix} m_2 q_2^2 + I_1 + I_2 & 0 \\ 0 & m_2 \end{bmatrix},$$

where m_2, I_1, and I_2 are the mass of link 2, inertia of link 1, and inertia of link 2, respectively. Note that $d_{11} = (m_2 q_2^2 + I_1 + I_2) \to \infty$ as $q_2 \to \infty$. Hence, there is no constant σ_2 such that (Equation 53.18) is satisfied for all possible values of q_2.

The class of robot manipulators for which the inertia matrix is uniformly bounded, hence satisfying Equation 53.18, are fully characterized in (Ghorbel et al. 1993) and is summarized here. The joint configurations of a robot manipulator which lead to a uniformly bounded inertia matrix satisfying Equation 53.18 are

1. All joints are prismatic ($\mathcal{P}\mathcal{P} \ldots \mathcal{P}\mathcal{P}$).
2. All joints are revolute ($\mathcal{R}\mathcal{R} \ldots \mathcal{R}\mathcal{R}$).
3. A series of prismatic joints followed by a series of revolute joints ($\mathcal{P}\mathcal{P} \ldots \mathcal{P}\mathcal{R} \ldots \mathcal{R}\mathcal{R}$).
4. Configurations where the axis of translation of each prismatic joint j is parallel to all preceding revolute joints k.

It was shown in Ghorbel et al. (1993) that for the above class of robot manipulators, the constants σ_1 and σ_2 can be explicitly determined in terms of the Denavit–Hartenberg kinematic parameters as well as the inertia link parameters.

EXAMPLE 53.2:

The two-link manipulator shown in Figure 53.61 consists of a prismatic joint followed by a revolute joint ($\mathcal{P}\mathcal{R}$). The kinematic (Denavit-Hartenberg) and dynamic link parameters are given in

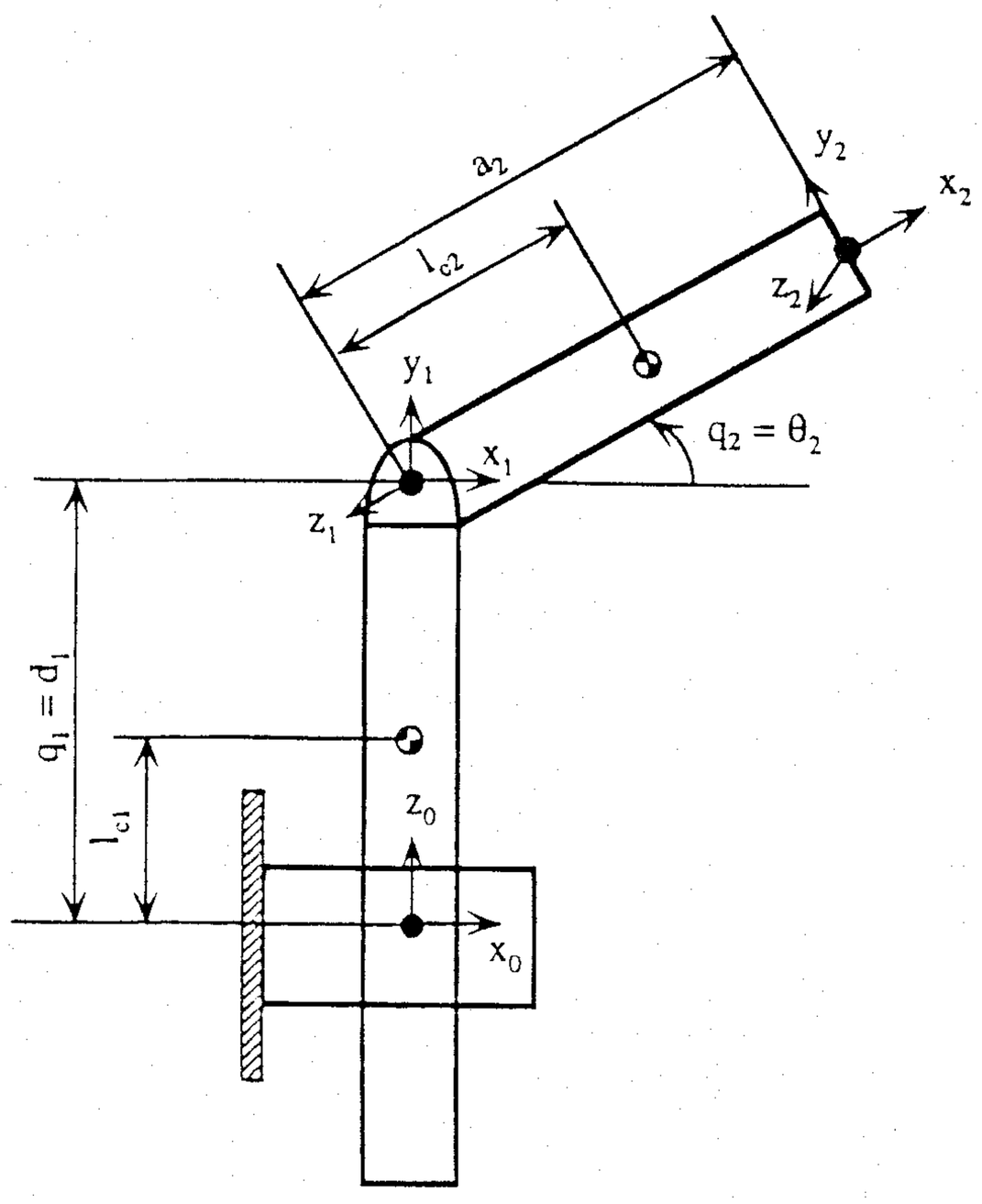

Figure 53.61 A two-link *PR* manipulator.

Table 53.1 Kinematic and Dynamic Link Parameters

Link i	Type	a_i	α_i	d_i	θ_i	q_i	m_i	l_{ci}	I_i
1	Prismatic	0	$\pi/2$	d_1	0	d_1	m_1	$d_1 - d_0$	diag $[I_{1x}\ I_{1y}\ I_{1z}]$
2	Revolute	a_2	0	0	θ_2	θ_2	m_2	l_{c2}	diag $[I_{2x}\ I_{2y}\ I_{2z}]$

Table 53.1 (see Spong and Vidyasagar (1989) for the definition of the Denavit–Hartenberg parameters a_i, α_i, d_i, and θ_i).

The inertia matrix is given by (Ghorbel et al. (1993))

$$D(\mathbf{q}) = \begin{bmatrix} m_1 + m_2 & m_2 l_{c_2} C_2 \\ m_2 l_{c_2} C_2 & m_2 l_{c_2}^2 + I_{2z} \end{bmatrix}.$$

Let $\bar{I}_2 = \max [I_{2x}, I_{2y}, I_{2z}]$. Then, the uniform bounds σ_1 and σ_2 of $D(\mathbf{q})$ are given by Ghorbel et al. (1993).

$$\sigma_1 = \frac{m_1(m_2 l_{c_2}^2 + I_{2z})}{m_1 + m_2(1 + l_{c_2}^2) + \bar{I}_2}$$

$$\sigma_2 = \frac{(m_1 + m_2(1 + l_{c_2}^2) + \bar{I}_2)^2 - m_1(m_2 l_{c_2}^2 + I_{2z})}{m_1 + m_2(1 + l_{c_2}^2) + \bar{I}_2}$$

For $m_1 = m_2 = 1$, $\bar{I}_2 = I_{2z} = 0.75$, $l_{c2} = 1$, we obtain $\sigma_1 = 0.47$, and $\sigma_2 = 3.28$.

Boundedness of the Derivative of the Gravity Vector

Another important boundedness inequality used in some of the control laws that are described in a later section concerns the derivative of the gravity vector. Specifically, it is typically assumed that a positive constant β exists such that

$$\left\| \frac{\partial \mathbf{g}(\mathbf{q})}{\partial \mathbf{q}} \right\| \leq \beta, \tag{53.19}$$

where the matrix norm

$$\left\| \frac{\partial \mathbf{g}(\mathbf{q})}{\partial \mathbf{q}} \right\| = \sqrt{\lambda_{\max}\left[\left[\frac{\partial \mathbf{g}(\mathbf{q})}{\partial \mathbf{q}} \right]^T \left[\frac{\partial \mathbf{g}(\mathbf{q})}{\partial \mathbf{q}} \right] \right]}.$$

It turns out that not all joint configurations insure the existence of a positive constant β such that inequality (Equation 53.19) is satisfied for all $\mathbf{q}$. A characterization of joint configurations of serial link robot manipulators for which inequality (Equation 53.19) is satisfied, and an explicit expression for β were recently proposed in Ghorbel and Gunawardana (1996) and Gunawardana and Ghorbel (1996).

Motion Control

Even though robot manipulators are very complex nonlinear systems, we show in this section how the structural properties just discussed can be exploited in a fundamental way to design control law strategies. First, we describe the design of PD-based

control laws for the regulation problem, that is, the following of a constant trajectory. We consider different cases including full and simple gravity compensation, and adaptive PD control for the class of robot manipulators with bounded inertia matrix. Second, we present an adaptive passivity based control law for the tracking of time varying desired trajectories. Third, we introduce the problem of joint flexibility of the manipulator and discuss an adaptive composite control law that compensates for the joint flexibility. An experimental case study is presented.

PD Control

The results presented in this section deal with the design of PD-based control laws for regulation in which the control objective is stated as follows: Given a constant desired joint trajectory, namely $\mathbf{q}_d(t) = \overline{\mathbf{q}}_d$ and $\dot{\mathbf{q}}_d = 0$, design a PD-based control law such that $\mathbf{q}(t) \to \overline{\mathbf{q}}_d$ and $\dot{\mathbf{q}}(t) \to 0$ as $t \to \infty$.

Absence of Gravity. In the absence of gravity, i.e., when $\mathbf{g}(\mathbf{q}) = 0$, the equations of motion (Equation 53.15) become

$$\text{Plant: } D(\mathbf{q})\ddot{\mathbf{q}} + C(\mathbf{q}, \dot{\mathbf{q}})\dot{\mathbf{q}} = \mathbf{u}. \tag{53.20}$$

The two-DOF manipulator in Figure 53.59 satisfies Equation 53.20 when the x-y plane is horizontal. Consider an independent joint PD control scheme

$$\text{Control Law: } \mathbf{u} = K_p(\overline{\mathbf{q}}_d - \mathbf{q}) - K_d\dot{\mathbf{q}}, \tag{53.21}$$

where K_p and K_d are diagonal matrices with positive entries. When the control law (Equation 53.21) is used for the plant (Equation 53.20), the equilibrium $\mathbf{q} = \overline{\mathbf{q}}_d$, $\dot{\mathbf{q}} = 0$ is globally asymptotically stable, that is, for any initial conditions $\mathbf{q}_0$, $\dot{\mathbf{q}}_0$, the trajectories of the plant satisfy $\mathbf{q}(t) \to \overline{\mathbf{q}}_d$ and $\dot{\mathbf{q}}(t) \to 0$ as $t \to \infty$.

This result is classic (see for example Spong and Vidyasagas, 1989) and an outline of the proof is as follows: First, Equations 53.20 and 53.21 are combined and evaluated at steady state, i.e., at $\ddot{\mathbf{q}} = 0$, $\dot{\mathbf{q}} = 0$, giving an equilibrium point $\mathbf{q} = \overline{\mathbf{q}}_d$ and $\dot{\mathbf{q}} = 0$. To show asymptotic stability of the equilibrium point, we choose the following Lyapunov function candidate:

$$V = \frac{1}{2}\dot{\mathbf{q}}^T D\dot{\mathbf{q}} + \frac{1}{2}(\overline{\mathbf{q}}_d - \mathbf{q})^T K_p(\overline{\mathbf{q}}_d - \mathbf{q}).$$

The time derivative of V along the solution trajectories of the closed loop system (53.20)–(53.21) is (after some algebra)

$$\dot{V} = -\dot{\mathbf{q}}^T K_d\dot{\mathbf{q}} + \frac{1}{2}\dot{\mathbf{q}}^T[\dot{D} - 2C]\dot{\mathbf{q}} = -\dot{\mathbf{q}}^T K_d\dot{\mathbf{q}} \leq 0,$$

where the skew symmetry property of $\dot{D} - 2C$ was used. It follows that the equilibrium $\mathbf{q} = \overline{\mathbf{q}}_d, \dot{\mathbf{q}} = 0$ is globally stable. Invoking LaSalle's theorem (Vidyasagar, 1993), global asymptotic stability is established.

Presence of Gravity but No-Gravity Compensation. Reconsider now the general case when gravity is present so that the equations of motion are given by Equation 53.15 and choose the (PD with no-gravity compensation) control law (Equation 53.21), that is,

$$\begin{cases} \text{Plant:} & D(\mathbf{q})\ddot{\mathbf{q}} + C(\mathbf{q}, \dot{\mathbf{q}})\dot{\mathbf{q}} + \mathbf{g}(\mathbf{q}) = \mathbf{u} \\ \text{Control law:} & \mathbf{u} = K_p(\overline{\mathbf{q}}_d - \mathbf{q}) - K_d\dot{\mathbf{q}}, \end{cases}$$

where K_p and K_d are diagonal matrices of positive entries. Assuming that the resulting closed loop system is stable, it follows that at steady state, i.e., at $\ddot{\mathbf{q}} = 0$, $\dot{\mathbf{q}} = 0$, we have

$$\overline{\mathbf{q}}_d - \mathbf{q} = K_p^{-1}\mathbf{g}(\mathbf{q}). \tag{53.22}$$

Consequently, we conclude that if no gravity compensation is added to the PD controller, there is always a steady state error given by Equation 53.22 which could be made smaller by choosing high gain K_p.

PD Control with Full Gravity Compensation. Adding full gravity compensation to the previous case, we obtain

$$\begin{cases} \text{Plant:} & D(\mathbf{q})\ddot{\mathbf{q}} + C(\mathbf{q}, \dot{\mathbf{q}})\dot{\mathbf{q}} + \mathbf{g}(\mathbf{q}) = \mathbf{u} \\ \text{Control law:} & \mathbf{u} = K_p(\overline{\mathbf{q}}_d - \mathbf{q}) - K_d\dot{\mathbf{q}} + \mathbf{g}(\mathbf{q}). \end{cases}$$

The control law actually cancels the effect of the gravitational terms. This gives the same closed loop system as the no-gravity case. Consequently we conclude that the equilibrium $\mathbf{q} = \overline{\mathbf{q}}_d$, $\dot{\mathbf{q}} = 0$ is globally asymptotically stable.

Note that the PD control law with full gravity compensation requires at each instant the computation of the gravitational terms in $\mathbf{g}(\mathbf{q})$. If the system parameters in $\mathbf{g}(\mathbf{q})$ are unknown, due for example to inaccuracy in measurement or change in payload, the global asymptotic stability of the equilibrium $\mathbf{q} = \overline{\mathbf{q}}_d$, $\dot{\mathbf{q}} = 0$, is no more achievable.

PD Control with Simple Gravity Compensation. It turns out that under further assumptions on the gravity vector, global asymptotic stability is still achievable without computing $\mathbf{g}(\mathbf{q})$ at each instant. Consider the following controller

$$\begin{cases} \text{Plant:} & D(\mathbf{q})\ddot{\mathbf{q}} + C(\mathbf{q}, \dot{\mathbf{q}})\dot{\mathbf{q}} + \mathbf{g}(\mathbf{q}) = \mathbf{u} \\ \text{Control law:} & \mathbf{u} = K_p(\overline{\mathbf{q}}_d - \mathbf{q}) - K_d\dot{\mathbf{q}} + \mathbf{g}(\overline{\mathbf{q}}_d). \end{cases}$$

Consider the class of robot manipulators, discussed earlier, for which inequality (Equation 53.19) is satisfied (Ghorbel and Gunawardana, 1996), that is, there is a constant β such that

$$\left\| \frac{\partial \mathbf{g}(\mathbf{q})}{\partial \mathbf{q}} \right\| \leq \beta.$$

If the elements k_{pi} of the diagonal matrix K_p are chosen such that $k_{pi} > \beta$, $1 \leq i \leq n$, and K_d is a diagonal matrix with positive

entries, then the equilibrium $\mathbf{q} = \bar{\mathbf{q}}_d$, $\dot{\mathbf{q}} = D$, is globally asymptotically stable, that is, $\mathbf{q}(t) \to \bar{\mathbf{q}}_d$ and $\dot{\mathbf{q}}(t) \to 0$ as $t \to \infty$ (Arimoto and Miyazeki, 1984; Korrami and Özgüner, 1988; Tomei, 1991).

Note that the difference between the full gravity compensation and the simple gravity compensation is that in the latter case the gravity term in the control law is computed at the desired position value $\bar{\mathbf{q}}_d$ only, hence it is constant and can be computed off-line. Therefore, the PD control law with simple gravity compensation doesn't require on-line model computation. Note that the result is valid only for the class of robot manipulators for which a constant β exists. Explicit expressions for β are discussed in Ghorbel and Gunawardana (1996). The proof of global asymptotic stability exploits in a fundamental way the skew symmetry of $\dot{D} - 2C$ and invokes LaSalle's Theorem (Vidyasagar, 1993).

Adaptive PD Control. For the class of robot manipulators with bounded inertia matrix for which there exist positive constants σ_1 and σ_2 satisfying Equation 53.18 (see Ghorbel et al., 1993, for full characterization of this class of robot manipulators and the computation of explicit bounds σ_1 and σ_2), an adaptive PD control law was proposed in Tomei (1991). Since the equations of motion are linear in the parameters as discussed earlier, the gravity vector can be expressed as $\mathbf{g}(\mathbf{q}) = Y_g(\mathbf{q})\Theta_g$ where the regressor matrix $Y_g(\mathbf{q})$ consists of known functions and the parameter vector Θ_g groups all the unknown parameters in $\mathbf{g}(\mathbf{q})$. Consider the following control law, and parameter update law

$$\begin{cases} \text{Plant:} & D(\mathbf{q})\ddot{\mathbf{q}} + C(\mathbf{q}, \dot{\mathbf{q}})\dot{\mathbf{q}} + \mathbf{g}(\mathbf{q}) = \mathbf{u} \\ \text{Control law:} & \mathbf{u} = K_p(\bar{\mathbf{q}}_d - \mathbf{q}) - K_d\dot{\mathbf{q}} + Y_g(\mathbf{q})\hat{\Theta}_g \\ \text{Parameter update law:} & \dot{\hat{\Theta}}_g = -\alpha Y_g^T(\mathbf{q})\left[\gamma\dot{\mathbf{q}} + \dfrac{2(\mathbf{q} - \bar{\mathbf{q}}_d)}{1 + 2(\mathbf{q} - \bar{\mathbf{q}}_d)^T(\mathbf{q} - \bar{\mathbf{q}}_d)}\right] \end{cases}$$

where α is a positive constant, K_p and K_d are constant diagonal matrices with positive entries, and γ satisfies

$$\gamma > \max\left\{\left[\frac{2\sigma_2}{\sqrt{\sigma_1\lambda_{\min[K_p]}}}\right], \left[\frac{1}{\lambda_{\min[K_d]}}\left(\frac{(\lambda_{\max[K_d]})^2}{2\lambda_{\min[K_p]}} + 4\sigma_2 + \frac{k_c}{\sqrt{2}}\right)\right]\right\}$$

where k_c is a constant that satisfies $\|C(\mathbf{q},\dot{\mathbf{q}})\| \leq k_c\|\dot{\mathbf{q}}\|$, $\lambda_{\min[K_p]}$ ($\lambda_{\min[K_d]}$) is the minimum eigenvalue of K_p (K_d) and $\lambda_{\max[K_p]}$ ($\lambda_{\max[K_d]}$) is the maximum eigenvalue of K_p (K_d). Then $(\mathbf{q}(t) - \bar{\mathbf{q}}_d)$, $\dot{\mathbf{q}}(t)$, and $\dot{\hat{\Theta}}_g(t)$ are bounded for $t \geq 0$. Moreover, $\mathbf{q}(t) \to \bar{\mathbf{q}}_d$ and $\dot{\mathbf{q}}(t) \to 0$ as $t \to \infty$ (Tomei 1991).

A Passivity-Based Control Law

In this section we present an adaptive passivity-based control law for the tracking problem in which the control objective is stated as follows: Given a desired joint trajectory, namely $\mathbf{q}_d(t)$, that is sufficiently many times continuously differentiable, design an adaptive control law such that $\mathbf{q}(t) \to \mathbf{q}_d(t)$ and $\dot{\mathbf{q}}(t) \to \dot{\mathbf{q}}_d(t)$ as $t \to \infty$ with all internal signals remaining bounded.

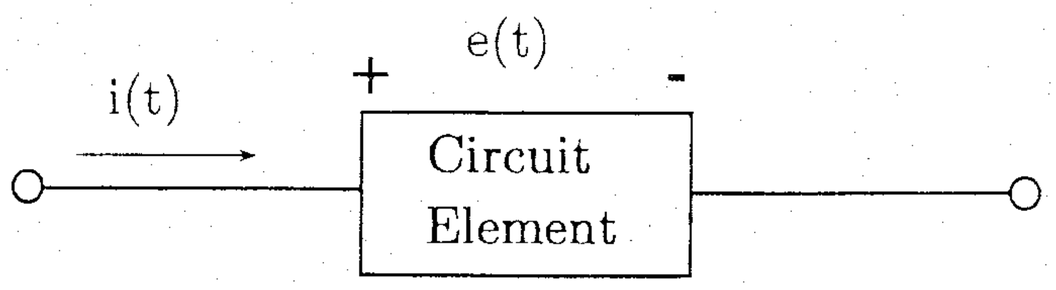

Figure 53.62 A circuit element.

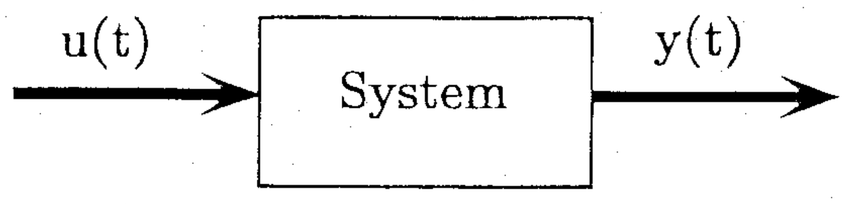

Figure 53.63 An input/output model.

Passivity. To introduce passivity, consider the circuit element shown in Figure 53.62 with positive current $i(t)$ and positive voltage $e(t)$. The power supplied to the element is $p(t) = e(t)i(t) \geq 0$. If at some instant $p(t)$ is negative, then the circuit element is supplying power to the rest of the circuit at that instance. Power is the time derivative of energy, hence the energy supplied to the circuit element over the interval time t_0 to t_1 is $\int_{t_0}^{t_1} p(t)dt = \mathscr{E}(t) - \mathscr{E}(t_0)$. Hence, the energy supplied to the circuit element at time t is $\mathscr{E}(t) = \mathscr{E}(t_0) + \int_{t_0}^{t_1} v(t)i(t)dt$. If $\mathscr{E}(t) \geq 0$ then energy is supplied to the system and we call the system *passive*. If, on the other hand, $\mathscr{E}(t) < 0$, the system supplies energy. For a mechanical system $p(t) = f(t)v(t)$ where $f(t)$ is force and $v(t)$ is velocity. It follows that $\mathscr{E}(t) = \mathscr{E}(t_0) + \int_{t_0}^{t_1} f(t)v(t)dt$. A mechanical system is passive if $\mathscr{E}(t) \geq 0$.

In a more general sense, consider the system shown in Figure 53.63 where the vector $\mathbf{u}(t)$ is the input to the system and the vector $\mathbf{y}(t)$ is the output. The system is said to be passive if $\int_0^\tau \mathbf{y}^T(t)\mathbf{u}(t)dt \geq -\gamma$ for all finite $\tau > 0$ and some finite $\gamma > 0$.

Passivity of Robot Manipulators. Consider the equations of motion of robot manipulators (Equation 53.15) which can be thought of as representing a system whose input is $\mathbf{u}$ and whose output is $\dot{\mathbf{q}}$. Then the equations of motion (Equation 53.15) define a passive mapping from the input $\mathbf{u}$ to the output $\dot{\mathbf{q}}$, that is $\int_0^\tau \dot{\mathbf{q}}^T(t)\mathbf{u}(t)dt \geq -\nu$ for some ν, and for all τ. This property is easily proved by considering the Hamiltonian of the system $\mathscr{H} = K + P$ which is the sum of the kinetic energy and the potential energy. Using the skew symmetry property of $\dot{D} - 2C$, it can easily be shown that $dH/dt = \dot{\mathbf{q}}^T\mathbf{u}$. Consequently, $\int_0^\tau \dot{\mathbf{q}}^T(t)\mathbf{u}(t)dt = H(T) - H(0) \geq -H(0)$ which proves the passivity property by setting $\nu = H(0)$.

A Passivity-Based Adaptive Control Law. Given a twice continuously differentiable reference trajectory $\mathbf{q}_d(t)$, consider the following control law

$$\mathbf{u} = \hat{D}(\mathbf{q})\mathbf{a} + \hat{C}(\mathbf{q}, \dot{\mathbf{q}})\mathbf{v} + \hat{\mathbf{g}}(\mathbf{q}) - K_D\mathbf{r}, \qquad (53.23)$$

where $\hat{D}$, $\hat{J}$, $\hat{C}$ and $\hat{\mathbf{g}}$ represent the terms in Equation 53.15 with estimated values of the parameters, K_D is a diagonal matrix of positive gains,

$$\tilde{\mathbf{q}} = \mathbf{q} - \mathbf{q}_d,$$

$$\mathbf{v} = \dot{\mathbf{q}}_d - \Lambda\tilde{\mathbf{q}},$$

$$\mathbf{r} = \dot{\mathbf{q}}_d - \Lambda\tilde{\mathbf{q}},$$

$$\mathbf{r} = \dot{\mathbf{q}} - \mathbf{v} = \dot{\tilde{\mathbf{q}}} + \Lambda\tilde{\mathbf{q}},$$

$$\mathbf{a} = \dot{\mathbf{v}},$$

and Λ is a constant diagonal matrix. Substituting Equation 53.23 into Equation 53.15, and since $\dot{\mathbf{q}} = \dot{\mathbf{r}} + \mathbf{a}$ and $\dot{\mathbf{q}} = \mathbf{r} + \mathbf{v}$, we can write the combined system as

$$\begin{aligned} D\dot{\mathbf{r}} + C\mathbf{r} + K_D\mathbf{r} &= \tilde{M}\mathbf{a} + \tilde{C}\mathbf{v} + \tilde{\mathbf{g}} \\ &= Y(\mathbf{q}, \dot{\mathbf{q}}, \mathbf{v}, \mathbf{a})\tilde{\boldsymbol{\Theta}}, \end{aligned} \tag{53.24}$$

where $\tilde{\Theta} = \hat{\Theta} - \Theta$ is the parameter error. Note that the regressor function Y in Equation 53.24 does not depend on the manipulator acceleration, but only on $\mathbf{v}$ and $\mathbf{a}$, which depend on the velocity and acceleration of the reference trajectory. The parameter update law is given by

$$\dot{\hat{\boldsymbol{\Theta}}} = -\Gamma Y^T\mathbf{r} \tag{53.25}$$

where Γ is some symmetric, positive definite matrix. The control law (Equation 53.23) and the parameter update law (Equation 53.25), namely,

$$\begin{cases} \text{Plant:} & D(\mathbf{q})\ddot{\mathbf{q}} + C(\mathbf{q}, \dot{\mathbf{q}})\dot{\mathbf{q}} + \mathbf{g}(\mathbf{q}) = \mathbf{u} \\ \text{Control Law:} & \mathbf{u} = \hat{D}(\mathbf{q})\mathbf{a} + \hat{C}(\mathbf{q}, \dot{\mathbf{q}})\mathbf{v} + \hat{\mathbf{g}}(\mathbf{q}) - K_D\mathbf{r} \\ \text{Parameter Update Law:} & \dot{\tilde{\Theta}} = -\Gamma Y^T\mathbf{r} \end{cases}$$

ensure the boundedness of all signals, preservation of passivity of the adaptive closed loop system, and the convergence of $\tilde{\mathbf{q}}$ and $\dot{\tilde{\mathbf{q}}}$ to zero, that is, $\mathbf{q}(t) \to \mathbf{q}_d(t)$ and $\dot{\mathbf{q}}(t) \to \dot{\mathbf{q}}_d(t)$.

This result can be proved by first showing that the mapping from input $-\mathbf{r}$ to output $Y\tilde{\Theta}$ is passive. Using expression (Equation 53.25), $\mathbf{r}^TY\tilde{\Theta} = -\dot{\tilde{\boldsymbol{\Theta}}}^{-1}\tilde{\boldsymbol{\Theta}}$, and hence,

$$\begin{aligned} -\int_0^\tau \mathbf{r}^TY\tilde{\boldsymbol{\Theta}}\,dt &= \int_0^\tau \dot{\tilde{\boldsymbol{\Theta}}}^T\Gamma^{-1}\tilde{\boldsymbol{\Theta}} \\ &= \frac{1}{2}\int_0^\tau \frac{d}{dt}[\tilde{\boldsymbol{\Theta}}^T\Gamma^{-1}\tilde{\boldsymbol{\Theta}}]\,dt \\ &= \frac{1}{2}\tilde{\boldsymbol{\Theta}}^T(\tau)\Gamma^{-1}\tilde{\boldsymbol{\Theta}}(\tau) - \frac{1}{2}\tilde{\boldsymbol{\Theta}}^T(0)\Gamma^{-1}\tilde{\boldsymbol{\Theta}}(0) \\ &\geq -\frac{1}{2}\tilde{\boldsymbol{\Theta}}^T(0)\Gamma^{-1}\tilde{\boldsymbol{\Theta}}(0) =: -\nu. \end{aligned}$$

Next we choose the Lyapunov function candidate V_1 defined by

$$\begin{aligned} V_1 &= \frac{1}{2}\mathbf{r}^TD\mathbf{r} + \tilde{\mathbf{q}}^T\Lambda^TK_D\tilde{\mathbf{q}} + \beta - \int_0^\tau \mathbf{r}^TY\tilde{\boldsymbol{\Theta}}\,dt \\ &= \frac{1}{2}\mathbf{r}^TD\mathbf{r} + \tilde{\mathbf{q}}^T\Lambda^TK_D\tilde{\mathbf{q}} + \frac{1}{2}\tilde{\boldsymbol{\Theta}}^T\Gamma^{-1}\tilde{\boldsymbol{\Theta}}. \end{aligned} \tag{53.26}$$

Using the skew symmetry property of $\dot{D} - 2C$, the time derivative of V_1 along the solution trajectories of Equation 53.24 can be shown to satisfy (after some algebra)

$$\dot{V}_1 = -\dot{\tilde{\mathbf{q}}}K_D\dot{\tilde{\mathbf{q}}} - \tilde{\mathbf{q}}\Lambda^TK_D\tilde{\mathbf{q}} \leq 0.$$

This proves stability, but additional arguments insure asymptotic stability (Ghorbel, 1990).

The above adaptive control law is due to Slotine and Li (1987). Note that it does not require acceleration measurement. Furthermore, the passivity property of the adaptive closed loop system is preserved which enabled us, using the Lyapunov function (Equation 53.26) along with the passivity property of the rigid robot, to conclude asymptotic stability.

Control of Flexible Joint Robot Manipulators

Joint Flexibility. A flexible joint robot model assumes that the actuators are elastically coupled to the links. The problem of joint flexibility, which arises from flexible couplings devices (harmonic drives, gear and bearing, fluid compressibility, etc.) between the rotor and the link, has been recognized as the major source of compliance in most present days manipulator designs. Experimental evidence (Sweet and Good, 1984) indicates that joint flexibility should be taken into account in both the modeling and control of manipulators if high performance is to be achieved. A model for flexible joint robot manipulators has been derived in Spong (1987) using the following assumptions:

- The kinetic energy of the rotor is due mainly to its own rotation. Equivalently, the motion of the rotor is a pure rotation with respect to an inertial frame.
- The rotor/gear inertia is symmetric about the rotor axis of rotation so that the gravitational potential of the system and also the velocity of the rotor center of mass are both independent of the rotor position.

Under the above assumptions, an n-link manipulator with revolute joints actuated by DC-electric motors and with elasticity of the joints modeled as linear torsional springs is suitably described by the following $2n$-dimensional set of differential equations (Spong, 1987):

$$D(\mathbf{q}_1)\ddot{\mathbf{q}}_1 + C(\mathbf{q}_1, \dot{\mathbf{q}}_1)\dot{\mathbf{q}}_1 + \mathbf{q}(\mathbf{q}_1) + K(\mathbf{q}_1 - \mathbf{q}_2) = 0 \tag{53.27}$$

$$J\ddot{\mathbf{q}}_2 - K(\mathbf{q}_1 - \mathbf{q}_2) = \mathbf{u}, \quad (53.28)$$

where the n-dimensional vectors $\mathbf{q}_1$ and $\mathbf{q}_2$ represent the link angles and rotor angles, respectively, $D(\mathbf{q}_1)$, $C(\mathbf{q}_1, \dot{\mathbf{q}}_1)\dot{\mathbf{q}}_1$, and $\mathbf{g}(\mathbf{q}_1)$ are as defined for the rigid model (Equation 53.15), J is a constant diagonal matrix of actuator inertias reflected to the link side of the gears, and K is a diagonal matrix representing the joint stiffness. For notational simplicity we will assume that all joint stiffness constants are the same in which case K may be taken as a scalar. In the limit as the joint stiffness K tends to infinity, we recover the n-dimensional rigid model (Spong, 1987).

$$[D(\mathbf{q}_1) + J]\ddot{\mathbf{q}}_1 + C(\mathbf{q}_1, \dot{\mathbf{q}}_1)\dot{\mathbf{q}}_1 + \mathbf{q}(\mathbf{q}_1) = \mathbf{u} \quad (53.29)$$

which is similar to the rigid model (Equation 53.15) in terms of $\mathbf{q}_1$.

It is easy to verify that of the four properties of rigid robot dynamics discussed earlier, positive definiteness $\begin{bmatrix} D(\mathbf{q}_1) & 0 \\ 0 & J \end{bmatrix}$ and uniform boundedness of its inverse, linearity in parameters, and skew symmetry of $d/dt\begin{bmatrix} D(\mathbf{q}_1) & 0 \\ 0 & J \end{bmatrix} - 2\begin{bmatrix} C & 0 \\ 0 & 0 \end{bmatrix}$ hold also in the case of flexible joint robots. The second property on the other hand fails to hold because the number of control inputs is n while there are $2n$ degrees of freedom.

It is easy to verify (even for a simple linear single-link arm) that the mapping $\mathbf{u} \rightarrow \dot{\mathbf{q}}_1$ (input $\rightarrow$ link velocity) is *not* passive. Consequently, the passivity based adaptive control law for rigid robots discussed earlier cannot be directly applied to flexible joint robots without further assumptions.

On the other hand, the dynamic Equations 53.27 and 53.28 of the flexible joint robot define a passive mapping $\mathbf{u} \rightarrow \dot{\mathbf{q}}_2$ (input $\rightarrow$ rotor velocity), i.e., $\int_0^\tau \dot{\mathbf{q}}_2^T(t)\mathbf{u}(t)dt \geq -\nu$ for some ν, and for all τ. This can be proved by defining the Hamiltonian $\mathcal{H}$ of Equations 53.27 and 53.28 which is the sum of the kinetic energy $K(\mathbf{q}, \dot{\mathbf{q}})$ and the potential energy $P(\mathbf{q})$

$$\begin{aligned}\mathcal{H} &= K + P \\ &= \frac{1}{2}\dot{\mathbf{q}}_1^T D(\mathbf{q}_1)\dot{\mathbf{q}}_1 + \frac{1}{2}\dot{\mathbf{q}}_2^T J\dot{\mathbf{q}}_2 + P_1(\mathbf{q}_1) \\ &\quad + \frac{1}{2}(\mathbf{q}_1 - \mathbf{q}_2)^T K(\mathbf{q}_1 - \mathbf{q}_2).\end{aligned}$$

It can be shown (Ghorbel, 1990) that $\int_0^\tau \dot{\mathbf{q}}_2^T \mathbf{u}dt = \int_0^\tau d\mathcal{H}/dt\, dt = \mathcal{H}(\tau) - \mathcal{H}(0) \geq -\mathcal{H}(0) =: -\nu$.

An implication of this fact is that we can directly apply the passivity-based adaptive control laws to control the rotor motion, and consider joint flexibility as unmodeled dynamics. But this would result in an accuracy problem since the control of link motion would become open loop, which is not acceptable for precision motion control.

It is clear that when the four properties discussed earlier are satisfied for rigid robots, they lead to a strong adaptive control result. On the other hand, the fact that the second property does not hold for the flexible joint case, and that the mapping $\mathbf{u} \rightarrow \mathbf{q}_1$ is not passive, greatly complicates the control problem of flexible joint robot manipulators.

Numerous approaches have been suggested in the literature for the control of flexible joint robot manipulators (Ghorbel, 1990). In this section, we only present one simple result based on singular perturbation method.

A Singular Perturbation Model For Flexible Joint Robots. We rewrite for convenience the dynamic Equations 53.27–53.28

$$D(\mathbf{q}_1)\ddot{\mathbf{q}}_1 + C(\mathbf{q}_1, \dot{\mathbf{q}}_1)\dot{\mathbf{q}}_1 + \mathbf{g}(\mathbf{q}_1) + K(\mathbf{q}_1 - \mathbf{q}_2) = 0 \quad (53.30)$$

$$J\ddot{\mathbf{q}}_2 - K(\mathbf{q}_1 - \mathbf{q}_2) = \mathbf{u}, \quad (53.31)$$

and define $\mathbf{z} := K(\mathbf{q}_2 - \mathbf{q}_1)$. The variable $\mathbf{z}$ therefore represents the torque transmitted through the joint. It is realistic to assume that the joint stiffness is large relative to other parameters in the system. We idealize the assumption of large joint stiffness by assuming that K is $O(1/\epsilon^2)$ where ϵ is a small parameter, so that we may write $K = 1/\epsilon^2 K_1$, where K_1 is $O(1)$.

The parameter ϵ can be interpreted as follows. First, it is obvious that ϵ is inversely proportional to the square root of the joint stiffness. The choice of the proportionality constant K_1 is dictated by design considerations. Roughly speaking, ϵ should be so that this proportionality constant is in the same range as other parameters (inertia, etc.) in the system. At the same time, ϵ should be small enough to ensure that the transient response of the boundary-layer system, defined in the following analysis, is sufficiently rapid.

Under the preceding assumptions, the dynamic Equations 53.30 and 53.31 are modified as follows:

$$D(\mathbf{q}_1)\ddot{\mathbf{q}}_1 + C(\mathbf{q}_1, \dot{\mathbf{q}}_1)\dot{\mathbf{q}}_1 + \mathbf{g}(\mathbf{q}_1) = \mathbf{z} \quad (53.32)$$

$$\epsilon^2 J\dot{\mathbf{z}} + K_1\mathbf{z} = K_1(\mathbf{u} - J\ddot{\mathbf{q}}_1). \quad (53.33)$$

In this form, we clearly see how the joint force drives the rigid links, and how the link motion can excite the joint resonance. The system of Equations 53.32 and 53.33 is a singular perturbation of the rigid robot model (Equation 53.29). The link positions and velocities are the "slow" variables while the joint torques and torque rates are the "fast" variables. Equation 53.33 represents the *fast system*. When $\epsilon = 0$, which corresponds to infinite joint stiffness, Equations 53.32 and 53.33 become

$$D(\bar{\mathbf{q}}_1)\ddot{\bar{\mathbf{q}}}_1 + C(\bar{q}_1, \dot{\bar{\mathbf{q}}}_1)\dot{\bar{\mathbf{q}}}_1 + \mathbf{g}(\bar{\mathbf{q}}_1) = \bar{\mathbf{z}} \quad (53.34)$$

$$K_1\bar{\mathbf{z}} = K_1(\mathbf{u} - J\ddot{\bar{\mathbf{q}}}_1) \quad (53.35)$$

where the overbar denotes that all the variables are computed at $\epsilon = 0$. From Equation 53.35 we obtain

$$\bar{\mathbf{z}} = \mathbf{u} - J\ddot{\bar{\mathbf{q}}}_1 \quad (53.36)$$

which, when substituted in Equation 53.34, yields the *slow reduced order system*

$$[D(\bar{\mathbf{q}}_1) + J]\ddot{\bar{\mathbf{q}}}_1 + C(\bar{\mathbf{q}}_1, \dot{\bar{\mathbf{q}}}_1)\dot{\bar{\mathbf{q}}}_1 + \mathbf{g}(\bar{\mathbf{q}}_1) = \mathbf{u} \qquad (53.37)$$

which is just the rigid model (Equation 53.29) in terms of $\bar{\mathbf{q}}_1$.

Composite Control From Equation 53.33, we observe that the joint resonant modes are purely oscillatory and this, in fact, is largely the source of the problem associated with joint flexibility in robot control. The composite control approach can be explained intuitively then as follows: a fast feedback control law is first designed to damp the oscillations of the fast variables. Once the fast transients have decayed, the slow part of the system should appear nearly like the dynamics of a rigid robot, which can then be controlled using any number of techniques. The idea of *composite control*, therefore, is to set

$$\mathbf{u} = \mathbf{u}_s(\mathbf{q}_1, \dot{\mathbf{q}}_1, t) + \mathbf{u}_f(\mathbf{z}, \dot{\mathbf{z}}). \qquad (53.38)$$

The term $\mathbf{u}_s$ is the *slow control*, and $\mathbf{u}_f$ is the *fast* control. Based on the previous decomposition of the flexible joint model, a reasonable choice for the fast control is

$$\mathbf{u}_f = K_v(\dot{\mathbf{q}}_1, \dot{\mathbf{q}}_2). \qquad (53.39)$$

We choose K_v as a constant diagonal matrix such that $K_v = O(1/\epsilon)$, that is,

$$K_v = \frac{1}{\epsilon} K_2, \qquad (53.40)$$

where K_2 is $O(1)$. Substituting the composite control (Equation 53.38) and the expression (Equation 53.40) into (Equations 53.32 and 53.33), we obtain

$$D(\mathbf{q}_1)\ddot{\mathbf{q}}_1 + C(\mathbf{q}_1, \dot{\mathbf{q}}_1)\dot{\mathbf{q}}_1 + \mathbf{g}(\mathbf{q}_1) = \mathbf{z} \qquad (53.41)$$

$$\epsilon^2 J\ddot{\mathbf{z}} + \epsilon K_2\dot{\mathbf{z}} + K_1\mathbf{z} = K_1(\mathbf{u}_s - J\ddot{\mathbf{q}}_1). \qquad (53.42)$$

It is important to note that the addition of the fast control (Equation 53.39) does not alter the slow system since at $\epsilon = 0$ the singularly perturbed system (Equations 53.41 and 53.42) reduces to (Equation 53.37). Thus the design of the slow control $\mathbf{u}_s$ is independent of the fast control. To control the slow reduced order system we now have two choices:

- We can use any number of techniques for the control of rigid robots to design the slow reduced order system. This will be presented briefly next. Details are found in Ghorbel (1990), Ghorbel and Spong (1990), and Ghorbel et al. (1989).
- We can use the integral manifold approach. In the integral manifold method, the slow control consists of the same rigid based component as above together with additional correction terms. This approach is not presented here. Details are found in Ghorbel and Spong (1992a,b; 1991) and Ghorbel (1990).

Using the adaptive passivity based algorithm of Slotine and Li (1987) discussed earlier for the design of the reduced order (rigid) system, the slow control and the parameter update law are therefore given by Equations 53.23 and 53.25 with $\mathbf{q} = \mathbf{q}_1$, that is,

$$\mathbf{u}_s = (\hat{D}(\mathbf{q}_1) + \hat{J})\mathbf{a} + \hat{C}(\mathbf{q}_1, \dot{\mathbf{q}}_1)\mathbf{v} + \hat{\mathbf{g}}(\mathbf{q}_1) - K_D\mathbf{r}, \qquad (53.43)$$

where now

$$\tilde{\mathbf{q}}_1 = \mathbf{q}_1 - \mathbf{q}_d,$$

$$\mathbf{v} = \dot{\mathbf{q}}_d - \Lambda\tilde{\mathbf{q}}_1,$$

$$\mathbf{r} = \dot{\mathbf{q}}_1 - \mathbf{v} = \dot{\tilde{\mathbf{q}}}_1 + \Lambda\tilde{\mathbf{q}}_1,$$

$$\mathbf{a} = \dot{\mathbf{v}},$$

and

$$\dot{\hat{\Theta}} = -\Gamma^{-1}Y^T\mathbf{r}. \qquad (53.44)$$

Using standard results from singular perturbation theory (Kokotović et al., 1986), we may approximate the system of Equations 53.41 and 53.42 by using a quasi-steady-state system and a boundary layer system as follows. Note that at $\epsilon = 0$, Equation 53.42 reduces to 53.36 which, when substituted into 53.41 yields Equation 53.37. The latter, which represents the rigid model Equation 53.29 in terms of $\bar{\mathbf{q}}_1$, is called the quasi-steady-state system. From Tichonov's theorem (Kokotević et al., 1986), the joint force $\mathbf{z}(t)$ and the link angle $\mathbf{q}_1(t)$ satisfy

$$\mathbf{z}(t) = \bar{\mathbf{z}}(t) + \eta(\tau) + O(\epsilon)$$

$$\mathbf{q}_1(t) = \bar{\mathbf{q}}_1(t) + O(\epsilon)$$

for $t > 0$, where $\tau = t/\epsilon$ is the fast time scale, $O(\epsilon)$ denotes terms of order ϵ and higher, and η satisfies the boundary layer equation

$$J\frac{d^2\eta}{d\tau^2} + K_2\frac{d\eta}{d\tau} + K_1(I + JD(\mathbf{q}_1)^{-1})\eta = 0.$$

It follows that the flexible joint system (Equations 53.41 and 53.42) can be written up to $O(\epsilon)$ as

$$D(\mathbf{q}_1)\ddot{\mathbf{q}}_1 + C(\mathbf{q}_1, \dot{\mathbf{q}}_1)\dot{\mathbf{q}}_1 + \mathbf{g}(\mathbf{q}_1) = \mathbf{u}_s + \eta(t/\epsilon) \qquad (53.45)$$

$$J\frac{d^2\eta}{d\tau^2} + K_2\frac{d\eta}{d\tau} + K_1(I + JD(\mathbf{q}_1)^{-1})\eta = 0. \qquad (53.46)$$

Substituting the control law (Equation 53.43) into Equation 53.45) and using the update law (Equation 53.44), the system

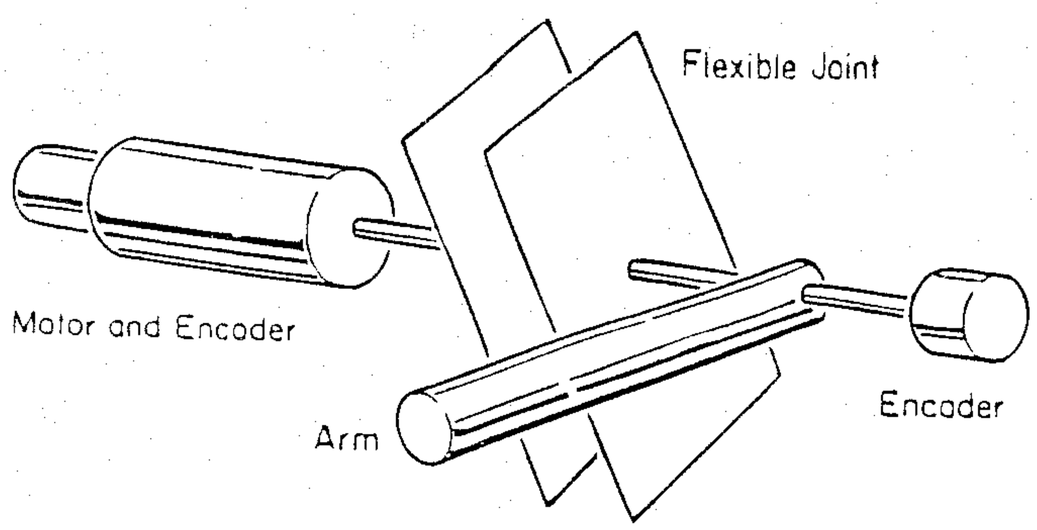

Figure 53.64 Sketch of experimental single-link flexible joint arm.

of Equations 53.45 and 53.46 can be written, after a little algebra, up to $O(\epsilon)$ as

$$M\dot{\mathbf{r}} + C\mathbf{r} + K_D\mathbf{r} = Y\tilde{\boldsymbol{\Theta}} + \eta(t/\epsilon) \quad (53.47)$$

$$J\frac{d^2\eta}{d\tau^2} + K_2\frac{d\eta}{d\tau} + K_1(I + JD(\mathbf{q}_1)^{-1})\eta = 0 \quad (53.48)$$

$$\dot{\hat{\boldsymbol{\Theta}}} = -\Gamma^{-1}Y^T\mathbf{r}. \quad (53.49)$$

We note that only the parameters of the rigid model are updated in this scheme. The joint stiffness and motor inertia need only be known with sufficient precision to determine K_2 to stabilize the boundary-layer system in the fast time scale. Typically these parameters can be identified with sufficient accuracy off-line and will not change with varying payloads.

The adaptive control scheme presented above has several attractive features with respect to its design and implementation. First, the overall complexity of the scheme is roughly the same as the rigid adaptive control scheme discussed earlier. Second, this control scheme exploits the two-time scale behavior in the system due to the relatively large joint stiffness, while, at the same time, it exploits the fundamental passivity properties of rigid robot dynamics. This is significant since the flexible joint robot dynamics do not possess the required passivity properties themselves as seen earlier. Third, the implementation of the full controller requires only joint position and velocity information. A detailed rigorous stability analysis of this scheme can be found in Ghorbel (1996) and Ghorbel and Spong (1990; 1989).

Example: An Experimental Single-Link Flexible Joint Arm. A single-link flexible joint arm is displayed in Figure 53.64 (Hung, 1989; Ghorbel et al., 1989). The flexible joint consists of two aluminum plates joined by extension springs. The actuator is a large DC motor connected directly to one plate. A hollow aluminum tube (1.5 inch diameter) about 18 inches long is connected to the second plate. Two incremental encoders provide feedback of the motor and link positions while velocity information is obtained by filtering the position feedback data. Parameter uncertainty is introduced by clamping payloads to the end of the arm. A payload that is approximately 40% of the nominal gravitational load of the arm is used in all experiments.

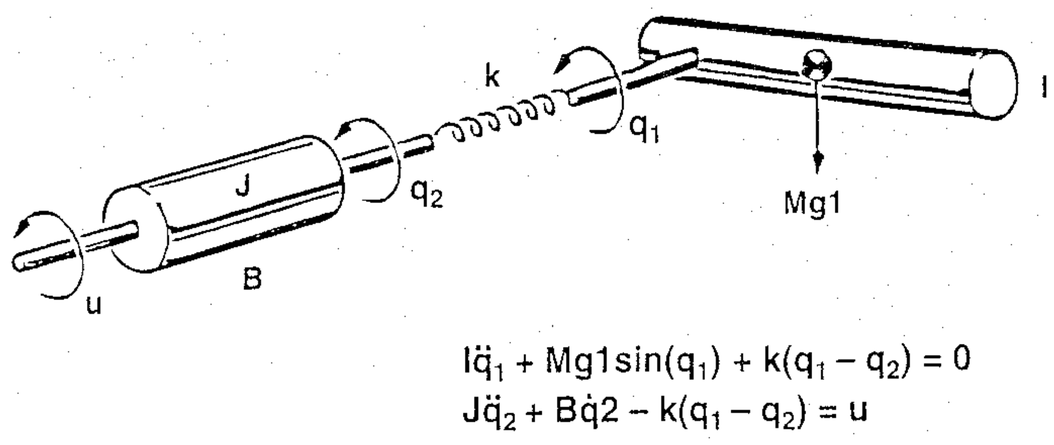

Figure 53.65 Model of experimental single-link flexible joint arm.

Table 53.2 Nominal Values of the Arm Parameters

Parameter	Value
Link inertia, I	0.031 $(kg - m^2)$
Rotor intertia, J	0.004 $(kg - m^2)$
Rotor friction, B_2	0.007 $(N - m - sec/rad)$
Nominal load, Mgl	0.8 $(N—m)$
Joint stiffness, k	7.13 $(N—m/rad)$

Table 53.3 Adaptive Composite Control System

Plant	$I\ddot{q}_1 + Mgl\sin(q_1) + k(q_1 - q_2) = 0$ $J\ddot{q}_2 + B_2\dot{q}_2 - k(q_1 - q_2) = u$
Control law	$u = u_s + u_f$ $u_f = K_v(\dot{q}_1 - \dot{q}_2)$ $u_s = \hat{\theta}_1 a + \hat{\theta}_2 sin(q_1) + B_2\nu - K_d\tau$
Parameter update law	$\dot{\hat{\theta}}_1 = -\gamma_1 a\tau$ $\dot{\hat{\theta}}_2 = -\gamma_2 sin(q_1)\tau$

The dynamics of this system are modeled as (Figure 53.65)

$$I\ddot{q}_1 + Mgl\sin(q_1) + k(q_1 - q_2) = 0$$

$$J\ddot{q}_2 + B_2\dot{q}_2 - k(q_1 - q) = u$$

Nominal values for the arm parameters without a payload are shown in Table 53.2. This system is of the form of Equations 53.30 and 53.31, except for the nonzero damping at the joint. However, as we will see, this damping is not sufficient to stabilize the elastic oscillation of the joint. The related rigid model, obtained in the limit as $k \to \infty$, is

$$(I + J)\ddot{q}_1 + B_2\dot{q}_1 + Mgl\sin(q_1) = u_s. \quad (53.50)$$

The coefficient B_2 is known with sufficient precision and hence we can simply cancel in the control law. Only the inertia parameters are affected by varying payloads. We invoke the third property of the rigid model (Equation 53.50) (see early section) and write

Table 53.4 Desired Trajectory

$q_d(t)$	A(rad)	α (rad/sec)
$A - Ae^{-\alpha t}(1 + \alpha t)$	$\pi/2$	5

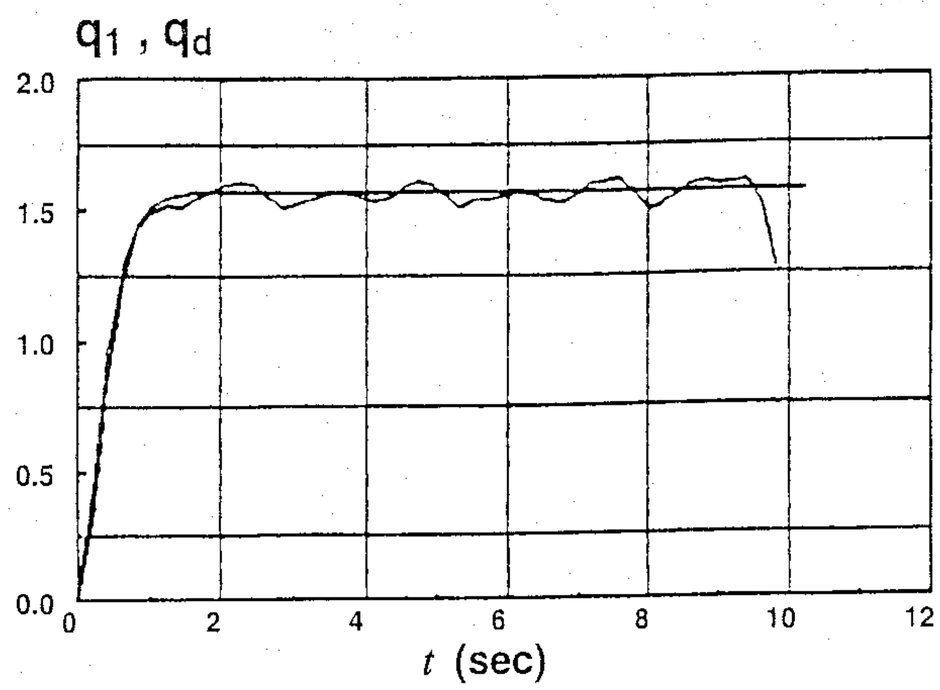

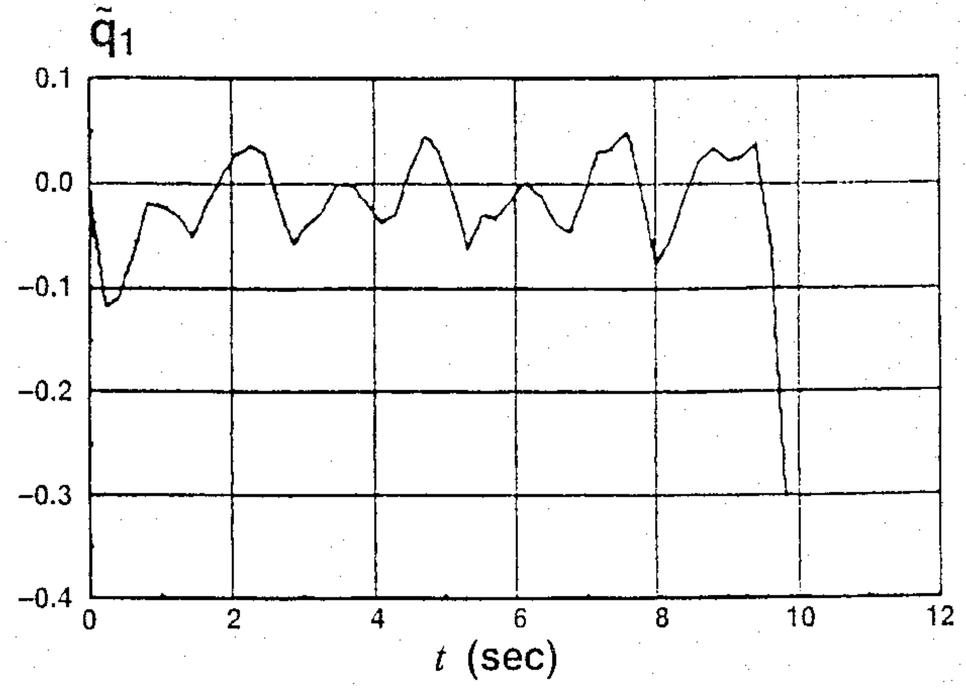

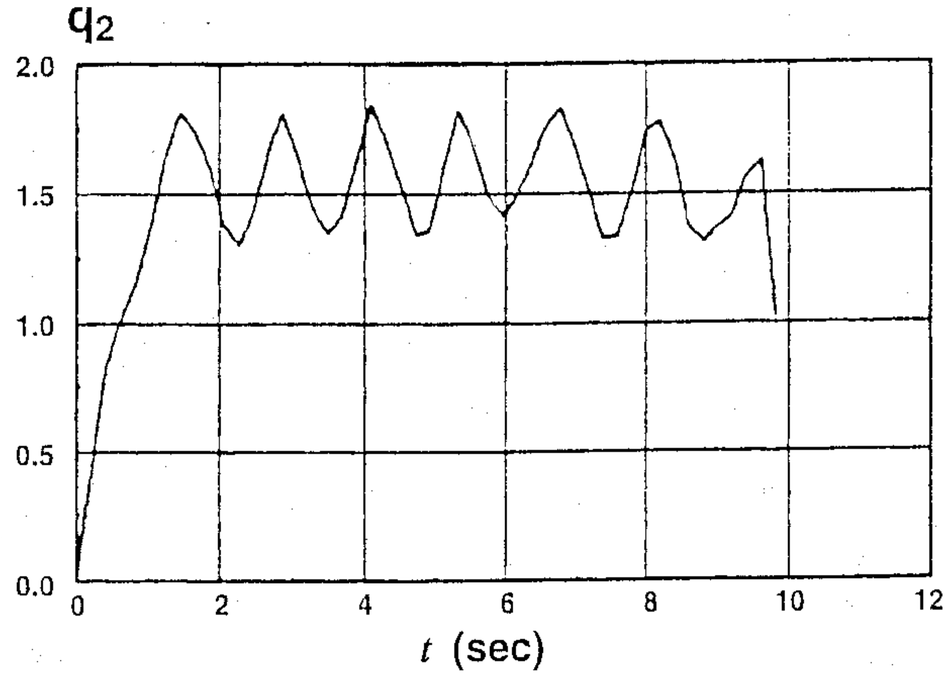

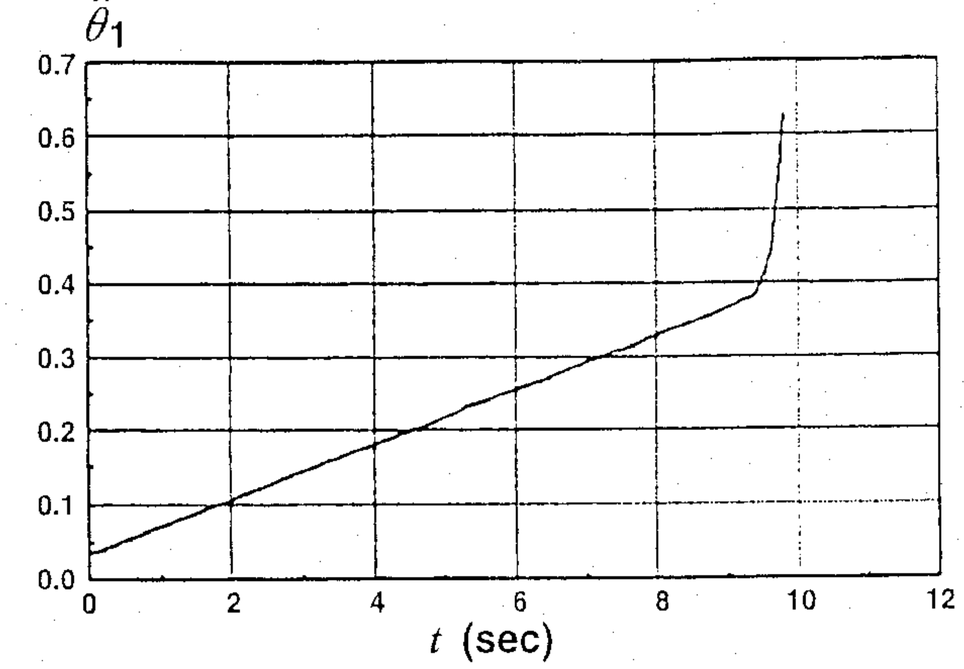

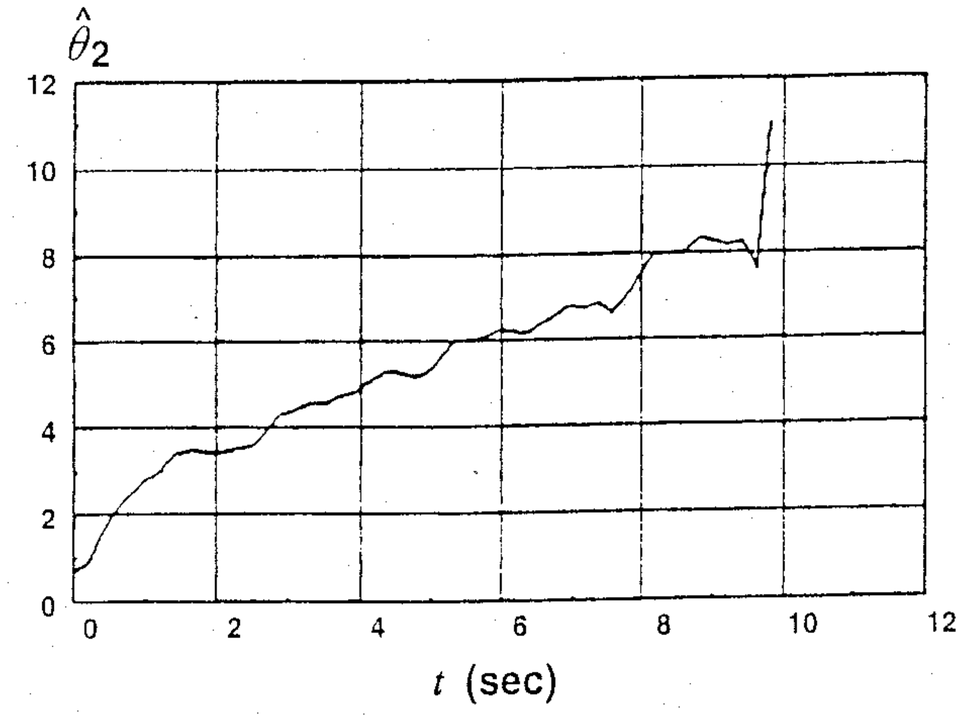

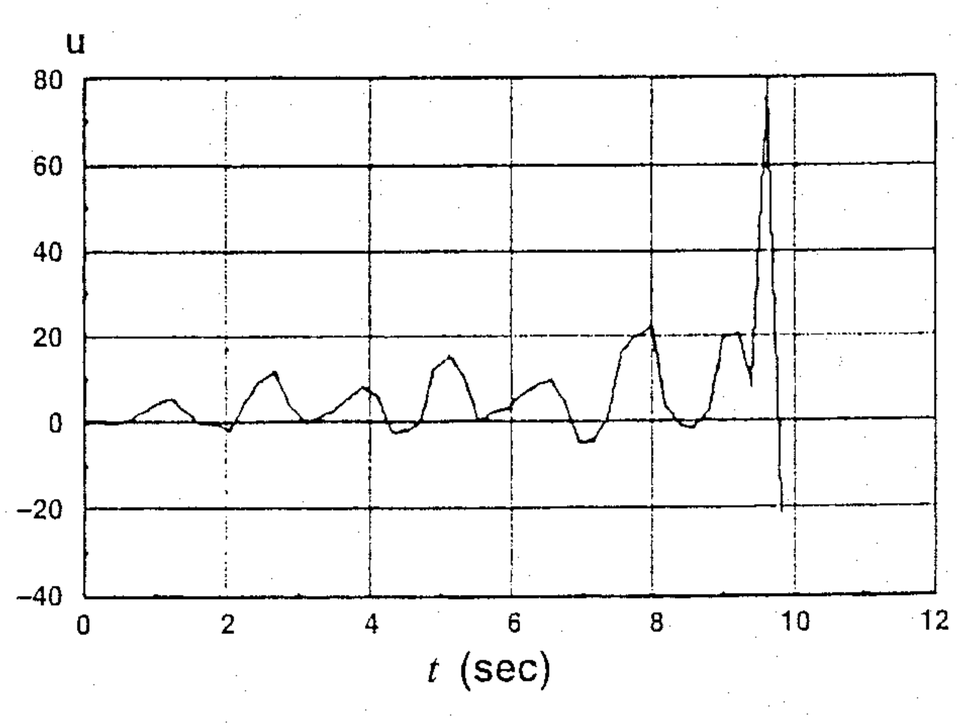

Figure 53.66 Response of flexible joint system with only adaptive rigid control.

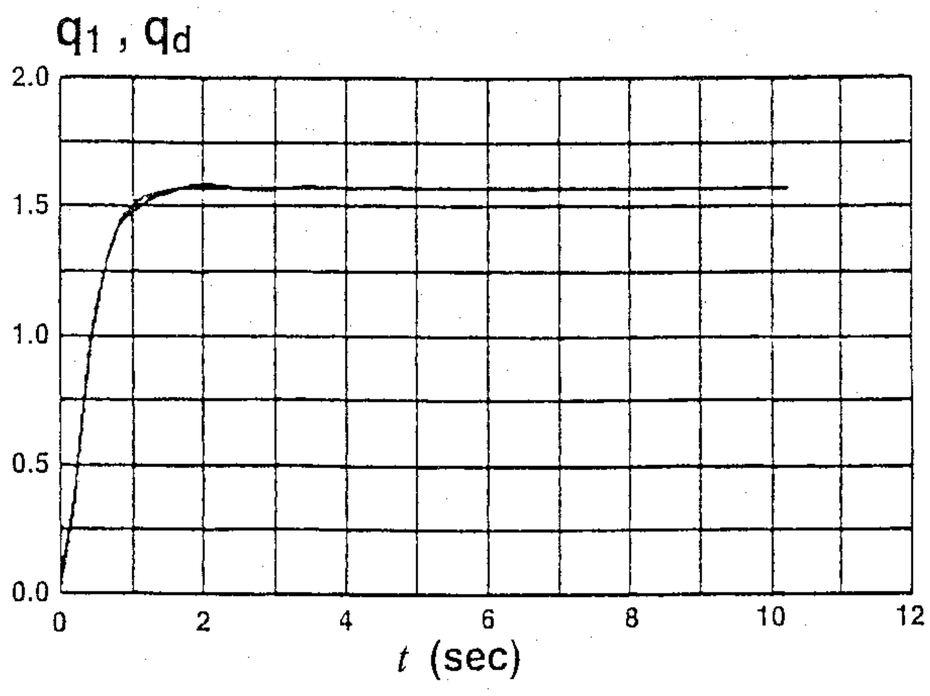

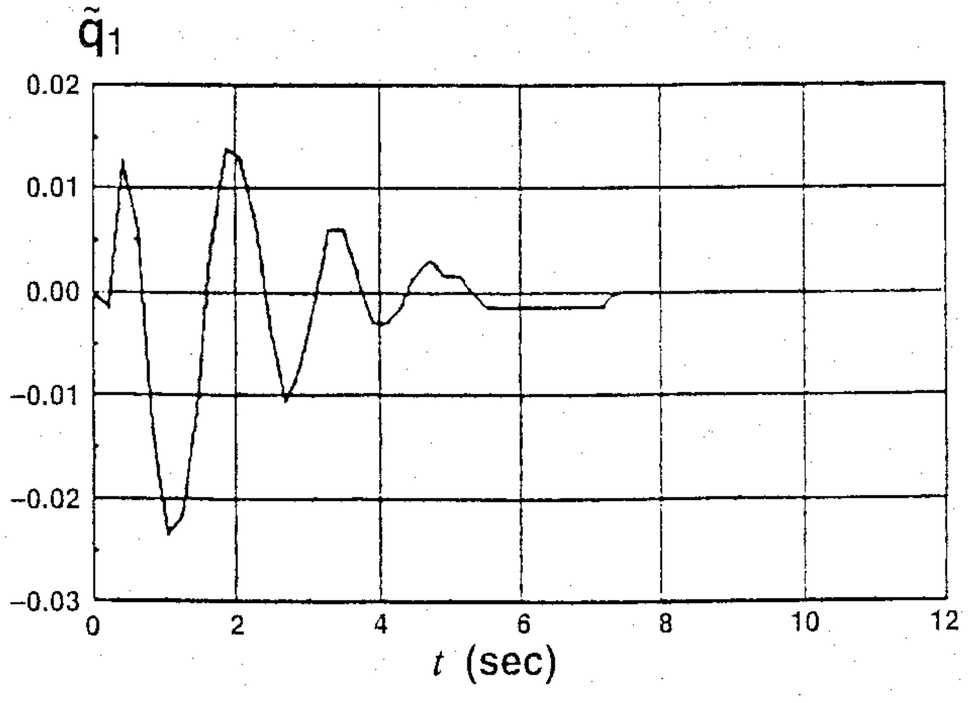

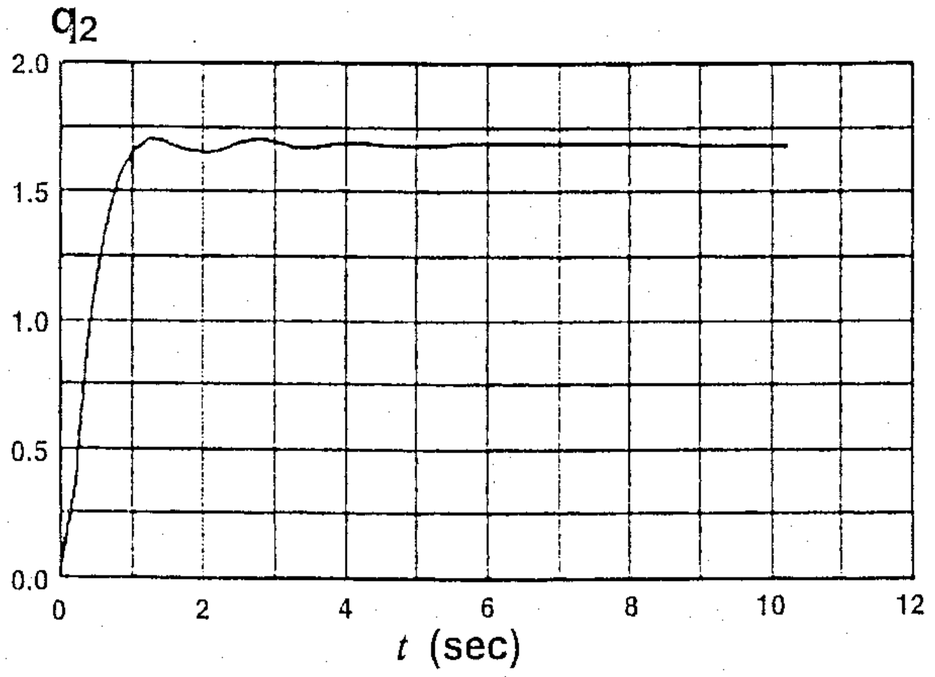

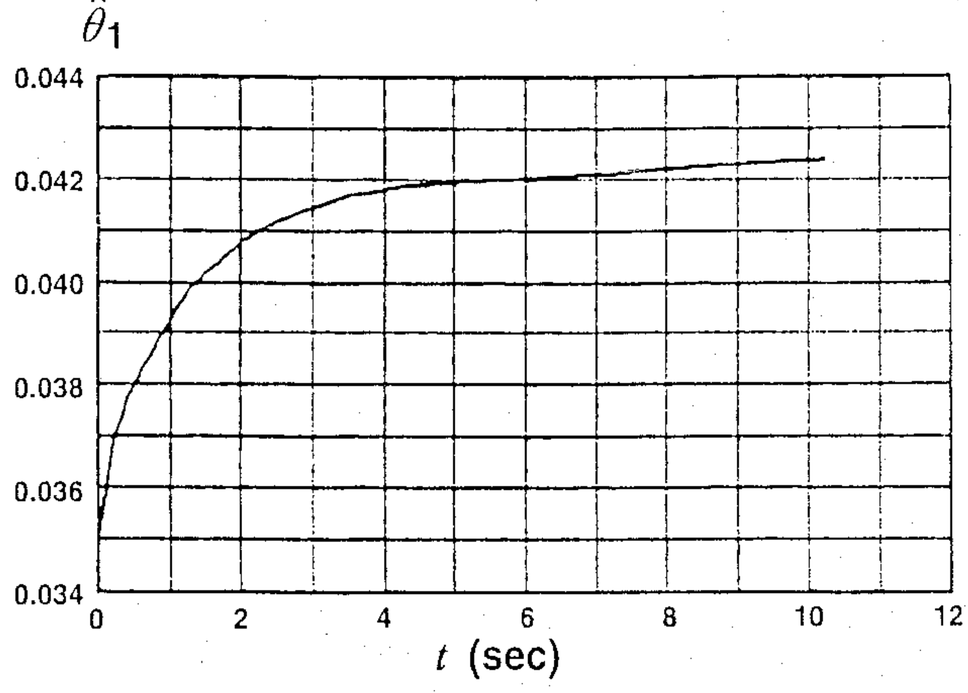

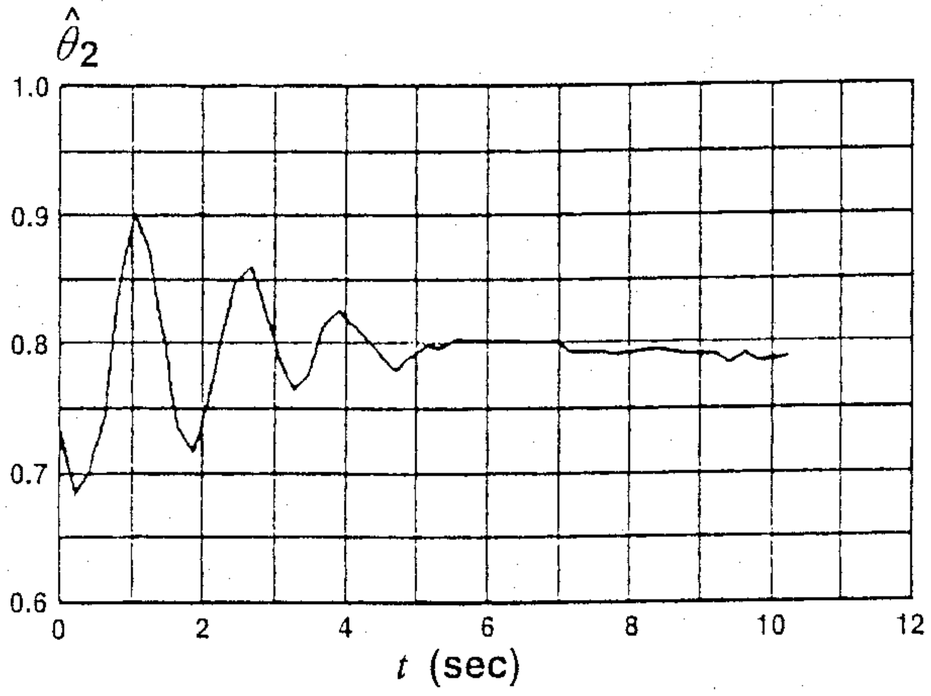

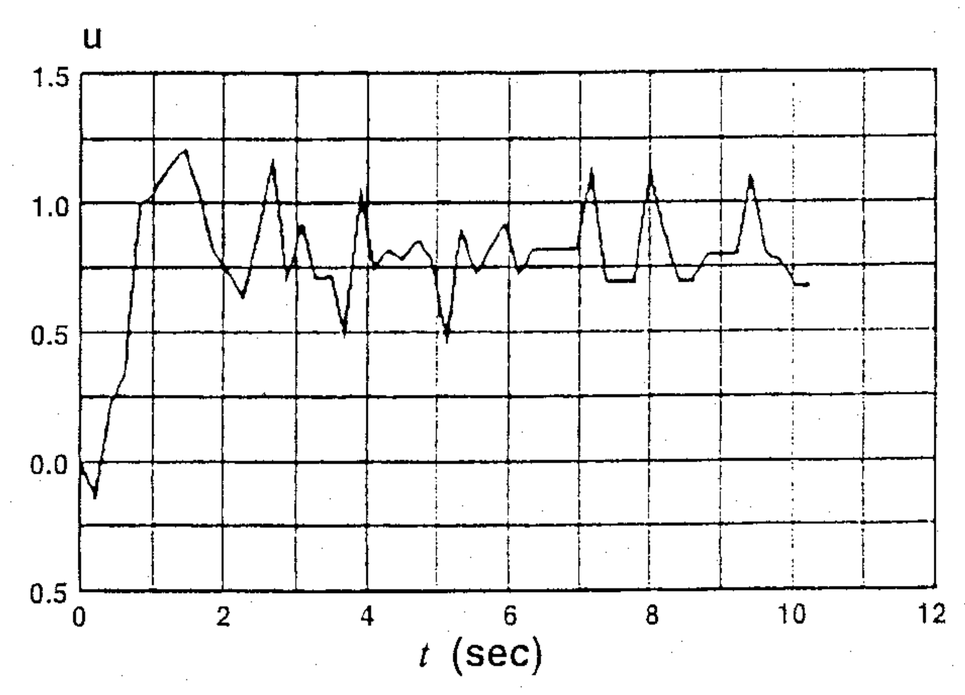

Figure 53.67 Response of flexible joint system with adaptive composite control.

$$(I + J)\ddot{q}_1 + B_2\dot{q}_1 + Mgl\sin(q_1) = Y\Theta + B_2\dot{q}_1$$
$$= u$$

$$\Theta = \begin{bmatrix}\theta_1\\ \theta_2\end{bmatrix} = \begin{bmatrix}I + J\\ Mgl\end{bmatrix},$$

$$Y = [\ddot{q}_1 \ \sin(q_1)].$$

The design of the rigid control law is now based on the rigid model (Equation 53.50). Using the passivity based adaptive control law for this term, the complete description of the control system is shown in Table 53.3. Recall that

$$\tilde{q}_1 = q_1 - q_d,$$

$$v = \dot{q}_d - \lambda\tilde{q}_1,$$

$$r = \dot{\tilde{q}}_1 + \lambda\tilde{q}_1,$$

$$a = \ddot{q}_d - \lambda\dot{\tilde{q}}_1,$$

where $q_d(t)$ is the desired trajectory.

An experiment was run to demonstrate the effectiveness of the composite control idea (Ghorbel, 1990; Ghorbel et al., 1989). A desired trajectory $q_d(t)$ consisting of a smooth 90-degree rotation with the arm initially pointing straight down is considered (Table 53.4). First, we neglect joint flexibility and use a rigid joint based adaptive control law (i.e., $u = u_s$, $u_f = 0$) with link variables for feedback. The result is an unstable system. Figure 53.66 displays the unsatisfactory response of the link. The response of the flexible joint system is bounded only because the joint deflection is limited by mechanical stops. The effectiveness of the adaptive composite control is shown in Figure 53.67 where the response is stable and the tracking is satisfactory. The gains used in the above two runs of the experiment are shown in Table 53.5.

Conclusions

In this section, we presented a sample of the recent control methods for the motion control of robot manipulators. We discussed the structural properties of the equations of motion and showed how they are exploited to facilitate the design of control laws. PD-based control laws with full and simple gravity compensation as well as adaptive PD controllers were discussed. An adaptive control law exploiting the passivity property of robot manipulators was also presented and its robustness with respect to joint flexibility was discussed. Finally, an adaptive composite control law based on singular perturbations methods was presented and tested using an experimental one link flexible joint manipulator.

Table 53.5 Gain Values for Experiment

Gain	λ	K_d	K_v	γ_1	γ_2
Adaptive rigid control only	10	1	0	0.001	5
Adaptive composite control	10	1	0.34	0.001	5

References

Abdallah, C., Dawson, D., Dorato, P., and Jamshidi, M. 1991. Survey of robust control for rigid robots, *IEEE Control Systems*, February, 24–30.

Arimoto, S. and Miyazaki, F. 1984. Stability and robustness of PID feedback control of robot manipulators of sensory capability, *1st Int. Symp. on Robotics Research*, M. Brady and R. P. Paul, eds., 783–799, MIT Press, Boston, MA.

Ghorbel, F., Hung, J. H., and Spong, M. W. 1989. Adaptive control of flexible joint manipulators, *IEEE Control System Magazine*, 9(7):9–13.

Ghorbel, F. and Spong, M. W. 1992. Robustness of adaptive control of robots, *J. Intelligent Robotic Systems*, 6:3–15. (Also published in *Symposium on the Control of Robots and Manufacturing Systems*, Arlington, Texas, November 9, 1990.)

Ghorbel, F. 1990. *Adaptive Control of Flexible Joint Robot Manipulators: A Singular Perturbation Approach*, Ph.D. Thesis, Department of Mechanical Engineering, University of Illinois, Urbana—Champaign, IL.

Ghorbel, F. and Spong, M. W. 1991. Integral manifold corrective control of flexible joint robot manipulators: the known parameter case, *Proc. ASME Winter Annual Meeting*, December 1–6, Atlanta, GA.

Ghorbel, F. and Spong, M. W. 1992a. Adaptive integral manifold corrective control of flexible joint robot manipulators, *Proc. 1992 IEEE Int. Conf. on Robotics and Automation*, May 10–15, Nice, France.

Ghorbel, F. and Spong, M. W. 1992b. Adaptive integral manifold control of flexible joint robots with configuration invariant inertia, *Proc. 1992 American Control Conf.* June 24–26, Chicago, IL.

Ghorbel, F., Srinivasan, B., and Spong, M. W. 1993. On the positive definiteness and uniform boundedness of the inertia matrix for robot manipulators, *Proc. 32nd IEEE Conf. on Decision and Control*, December 15–17, San Antonio, TX.

Ghorbel, F. and Gunawardana, R. 1996. A Uniform bound for the jacobian of the gravitational force vector for a class of robot manipulators, *ASME Journal of Dynamic Systems, Measurement, and Control*, (to appear, accepted April 1996).

Greenwood, D. T. 1977. *Classical Dynamics*, Prentice Hall, Englewood Cliffs, NJ.

Gunawardana, R. and Ghorbel, F. 1996. The class of robot manipulators with bounded jacobian of the gravity vector, *Proc. of the IEEE International Conference on Robotics and Automation*, Minneapolis, Minnesota, April 22–28, 1996.

Hung, J. Y. 1989. *Robust Control of Flexible Joint Robot Manipulators*, Ph.D. Thesis, Department of Electrical and Computer Engineering, University of Illinois, Urbana-Champaign, IL.

Kokotović, P. V., Khalil, H. K., and O'Reilly, J. 1986. *Singular Perturbation Methods in Control: Analysis and Design*, Academic Press, London, UK.

Korrami, F. and Özgüner, U. 1988. Decentralized control of robot manipulators via state and proportional-integral feedback, *IEEE Conf. Robotics and Automation,* 1198–1203, Philadelphia, PA.

Lewis, F. L., Abdallah, C. T., and Dawson, D. M. 1993. *Control of Robot Manipulators,* Macmillan, New York, NY.

Ortega, R. and Spong, M. W. 1988. Adaptive motion control of rigid robots: a tutorial, *Proc. 27th Conf. Decision and Control,* 1575–1584, Austin, TX.

Slotine, J.-J. E., and Li, W. 1987. On the adaptive control of robot manipulators, *Int. J. Robotics Research,* 6(3):49–59.

Spong, M. W., Lewis, F. L., and Abdallah, C. T. 1993. *Robot Control, Dynamics, Motion Planning, and Analysis,* IEEE Press, New York, NY.

Spong, M. W. and Vidyasagar, M. 1989. *Robot Dynamics and Control,* John Wiley and Sons, New York, NY.

Spong, M. W. 1987. Modeling and control of elastic joint manipulators, *J. Dyn. Sys., Meas. and Control,* 109:310–319.

Sweet, L. M. and Good, M. C. 1984. Redefinition of the robot motion control problem: effects of plant dynamics, drive system constraints, and user requirements, *Proc. 23rd IEEE CDC,* Las Vegas, NV.

Tomei, P. 1991. Adaptive PD controller for robot manipulators, *IEEE Trans. Robotics and Automation,* 7(4).

Vidyasagar, M. 1993. *Nonlinear Systems Analysis,* 2nd ed., Prentice Hall, Englewood Cliffs, NJ.

53.8 Mobile Robots

Miguel A. Salichs, Luis Moreno, Diego Gachet, Arthuro de la Escalera, Juan R. Pimentel

Introduction

The objective of this section is to provide a brief overview of industrial mobile robots. Currently, the primary types of mobile robots are legged and wheeled. However, the industrial applications of the former type are limited, thus, we only address wheeled robots. The style of the presentation consists of presenting the main issues and important results corresponding to a major mobile robot topic. No attempt is made in deriving formulas or presenting related theory or algorithms. The choice of topics was dictated by the practical nature of the section. Some topics (e.g., manipulators) were not treated extensively as they are covered in traditional robots as opposed to mobile robots. Because of space considerations, some topics that some readers might expect to find in this section were not considered.

Robot Platforms

Frame

The frame is usually constructed of welded steel members with aluminum or plastic cover plates. Mobile robots designed to operate in industrial areas or indoors do not have suspension systems.

Base

Many mobile robots designed for handling industrial loads have rectangular bases. This kind of base presents more restrictions to movements than circular bases because of the different longitudinal and transversal dimensions.

Vehicles with circular bases are appropriate for cluttered environments because the circular base minimizes the size of the vehicle in a given working area. The main advantage is that space is better utilized when compared to mobile robots with rectangular bases. Because of the nature of its base, mobile robots with circular bases have maximum maneuverability.

Steering Configuration

The types of wheels used in mobile robots can be classified as follows: driving, steering, driving and steering, and passive. Depending on the physical arrangement of the wheels and the types of wheels used, it is possible to have different kinematic and dynamic characteristics, as well as different motion behaviors.

Vehicles are designed to maneuver in different ways; depending on the requirements, it is possible to select from several drive configurations (Figure 53.68). Of course the drive configurations must be compatible with the vehicle base.

Tricycle. The driving action can be through the front wheel and/or the rear wheels with the steering action being done by the front wheel. The minimum radius of curvature (defined as the ratio of linear speed over angular speed) depends on the distance between the front and rear axles. The tricycle configurations is normally used for forward motion. From the motion point of view, mobile robots with carlike configuration have similar capabilities.

Differential. Differentially steered vehicles have two

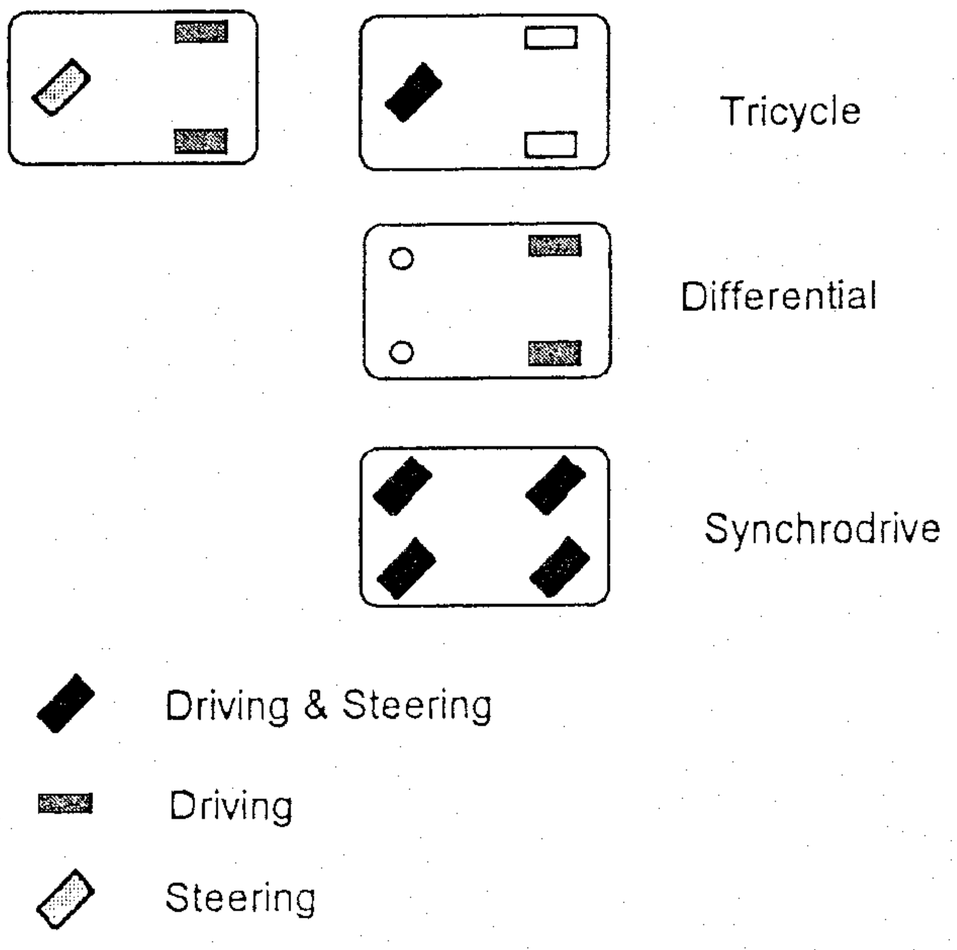

Figure 53.68 Steering configuration for mobile robots.

drive wheels which are responsible for driving and steering. The steering action is accomplished by having each wheel to rotate at different speeds. This type of configuration provides some additional advantages like forward and backward movements which can be performed at the same speed. In addition, the vehicle requires a smaller area to maneuver.

Synchrodrive. This technique, also known as all-wheel steering, has four steering wheels (two or four are also driving wheels). This configuration allows the vehicle to move transversally and a diagonal movement is also possible.

Manipulators

Depending on the mobile robot applications, there is a wide range of possible manipulation equipment on board the robot. If the application deals with material handling, the required tasks basically involve loading and unloading. For these types of applications, mobile robots have telescopic forks, conveyors or simply a platform.

Other applications require some kind of manipulation and these mobile robots include robotic manipulators on board. Such configuration needs additional control hardware for controlling the robot arm. Robot arms can be controlled in various ways: some difficult tasks need to be teleoperated and others can be done autonomously. In any case, it is necessary to collect appropriate sensory information form the environment.

Power

Mobile robots are typically powered by 24 or 48 V DC industrial batteries. Amp-hour requirements vary according to the mobile robot characteristics and the application.

There are two big groups of techniques for battery charging: opportunistic and full-cycle charging.

Opportunistic Charging. The opportunistic-charging technique involves the batteries being charged while the vehicle is waiting to perform (or is performing) a task. Time intervals during which the vehicle is stopped become possible charging intervals. The charge is done by means of a charging collector mounted on the vehicle that lowers the collector brushes to contact the floor-charger bus-plate. This charging method admits the use of maintenance free batteries.

Full-Cycle Charging. The full-cycle charging technique requires that the mobile robot be out of service and to go into a special battery-charging area. This is done when the battery is nearly discharged. There exists several charging methods for full-cycle charging.

Probe-type charging. In this technique the vehicle drives into a probe unit connected to an appropriate battery charger.

Bus-bar charging. The vehicle inserts its charging mast into a charging track connected to ac main supply and the charger is located on-board the vehicle.

Manuall Plug-in charging. The mobile robot is plugged in by an operator.

Change Out. If the mobile robot requires continuous service a battery exchange is the best solution, because it is much less expensive to have spare battery packs than to have spare vehicles.

Communications

Radio frequency communications is widely used for continuous communication. This technique allows different possibilities—the traditional one uses radio technology to establish a serial link between the ground station and the mobile robot (RS-232). Another possibility is to use the radio to create a Local Area Network. If the mobile robot is going to operate in indoor environments (hospitals, factories, etc.), it is also possible to use infrared links to communicate the mobile robot with the ground station or other vehicles.

In some situations, it can be desirable to send images to the ground station this could arise for instance if some operation requires teleoperation or operator decisions. These images can be sent through the conventional communication channels, which requires some kind of image compression, or can be communicated through a specific video communication channel.

Kinematics

To control a mobile robot, it is important to know the relationships between the actions on the actuators (e.g., linear and angular speed commands) and the movements of the robot. These relationships are used for two purposes. First to calculate the actions necessary to move the robot from one position to another. Second, to evaluate the displacements of the robot from the movements of the wheels (i.e., odometry).

In the following, we provide the kinematics equations that correspond to each of the steering configurations described in the section on robot platforms.

The driving signals are the steering wheel angle α and the linear speed of the driving wheel v, usually the front one (Figure 53.69). The kinematics equations of a point placed in the front wheel are

$$\dot{x}_F = -v \sin(\theta + \alpha)$$

$$\dot{y}_F = v \cos(\theta + \alpha)$$

$$\dot{\theta} = \frac{v}{L} \sin(\alpha)$$

The kinematics equations of a point placed in the middle of the rear axis are

$$\dot{x}_R = -v \cos(\alpha)\sin(\theta)$$